PNAS 2015-09213R

Stress-induced gene expression and behavior are controlled by DNA methylation and methyl donor availability in the dentate gyrus

Emily A. Saunderson[1], Helen Spiers[3], Karen R. Mifsud[1], Maria Gutierrez-Mecinas[1], Alexandra F. Trollope[1], Abeera Shaikh[1], Jonathan Mill[2, 3], Johannes M.H.M. Reul[1]*

[1]Neuro-Epigenetics Research Group, University of Bristol, Bristol BS1 3NY, UK

[2]University of Exeter Medical School, University of Exeter, Exeter EX2 5DW, UK

[3]Institute of Psychiatry, King's College London, London SE5 8AF, UK

Correspondence:
Professor Johannes M.H.M. Reul
Mail: Hans.Reul@bristol.ac.uk
Phone: +44 117 331 3137

Running title: DNA methylation and stress-induced IEGs and behavior

Classification: Biological Sciences (Major); Neuroscience (Minor)

Present addresses: A.F.T.: James Cook University, Townsville, QLD 4811, Australia; M.G.-M.: University of Glasgow, Glasgow G12 8QQ, UK

Abstract

Stressful events evoke long-term changes in behavioral responses; however the underlying mechanisms in the brain are not well understood. Previous work has shown that epigenetic changes and immediate-early gene (IEG) induction in stress-activated dentate gyrus (DG) granule neurons play a crucial role in these behavioral responses. Here we show that an acute stressful challenge, i.e. forced swimming, results in DNA demethylation at specific CpG sites close to the c-*Fos* transcriptional start site and within the gene promoter region of *Egr*-1 specifically in the DG. Administration of the (endogenous) methyl donor s-adenosyl methionine (SAM) did not affect CpG methylation and IEG gene expression at baseline. However, administration of SAM before the forced swim challenge resulted in an enhanced CpG methylation at the IEG loci and suppression of IEG induction specifically in the DG and an impaired behavioral immobility response 24 h later. The stressor also specifically increased the expression of the *de novo* DNA methyltransferase Dnmt3a in this hippocampus region. Moreover, stress resulted in an increased association of Dnmt3a enzyme with the affected CpG loci within the IEG genes. No effects of SAM were observed on stress-evoked histone modifications including H3S10p-K14ac, H3K4me3, H3K9me3 and H3K27me3. We conclude that the DNA methylation status of IEGs plays a crucial role in FS-induced IEG induction in DG granule neurons and associated behavioral responses. In addition, the concentration of available methyl donor, possibly in conjunction with Dnmt3a, is critical for the responsiveness of dentate neurons to environmental stimuli in terms of gene expression and behavior.

Keywords: Stress, behavior, c-Fos, Egr-1, DNA methylation, epigenetics, hippocampus

Significance statement

Appropriate behavioral responses to psychologically stressful events are important for maintaining mental health and wellbeing. The consolidation of these behavioral responses critically depends on the induction of the immediate-early gene products c-Fos and Egr-1 in dentate gyrus neurons. In this report, we found that an intricate balance between DNA methylation, DNA demethylation and availability of the methyl donor SAM governs the induction of these genes as well as the behavioral responses after stress. These findings provide new insights into the epigenetic control of gene expression underlying stress-induced behavioral adaptation.

\body

Introduction

Adaptation to stressful challenges is crucial for maintaining health and wellbeing. These events induce physiological and behavioral responses that enable the individual to cope with the challenge. In the brain, molecular mechanisms are initiated that facilitate learning of adaptive behavioral responses and the consolidation of memories of the event. Inappropriate responses to stress have been linked with psychiatric disorders such as major depression and anxiety (1-3).

Glucocorticoid hormones, secreted in response to a stressful challenge, in conjunction with activated intracellular signaling pathways in neurons of the hippocampus play a key role in consolidating behavioral responses to stress (4, 5). The hippocampal extracellular signal-regulated kinase mitogen-activated protein kinase (ERK MAPK) pathway, activated through N-methyl D-aspartate receptors (NMDA-Rs) and other membrane receptors, is involved in behavioral responses seen in Morris water maze learning, contextual fear conditioning and the forced swim test. In these behavioral paradigms, phosphorylated ERK1/2 in hippocampal neurons activate the chromatin-modifying enzymes MSK1 (mitogen- and stress-activated kinase 1) and Elk-1 (ETS domain protein 1) resulting in changes in gene transcription (5-7). Glucocorticoid hormones, via the glucocorticoid receptor (GR), facilitate the activation (phosphorylation) of MSK1 and Elk-1 by ERK1/2. MSK1 and Elk-1 activation lead to phosphorylation of serine-10 and acetylation of lysine-14, respectively, in histone H3 in multiple gene promoters, such as *c-Fos* and *Egr-1* (early growth response protein 1), resulting in transcriptional activation of these genes (5, 7). Blocking NMDA-Rs or GRs, inhibition of ERK MAPK signaling or gene deletion of MSK1 all prevent histone H3 phosphorylation and acetylation and the induction of c-Fos and Egr-1 in the hippocampus and impair behavioral responses in the Morris water maze test, contextual fear conditioning and the forced swim test (5, 8-12). Regarding the

forced swim test, the dentate gyrus (DG) was identified as the hippocampal region conferring these molecular and behavioral responses (4, 5, 11).

In addition to histone H3 phosphorylation and acetylation other epigenetic mechanisms including histone methylation and DNA methylation are thought to be involved in behavioral responses to stress. Acute and chronic restraint stress evokes distinct effects in histone H3 methylation in various sub-regions of the hippocampus (13). Contextual fear conditioning results in histone H3 methylation (e.g. di-methylation of lysine-9 (K9) or tri-methylation of K4 in histone H3) and DNA methylation changes in the hippocampus (13-16). Although c-Fos and Egr-1 gene induction have been shown to be of critical importance for the consolidation of behavioral responses in the Morris water maze, fear conditioning and forced swimming (FS) (5, 9, 17), the role of histone and DNA methylation changes at these immediate-early genes is still unclear. Interestingly, administration of the endogenous methyl donor S-adenosyl methionine (SAM) disrupts the consolidation of behavioral responses in the forced swim test (18) suggesting a requirement of methylation-dependent epigenetic mechanisms. Therefore, we postulated that in addition to histone H3 phosphorylation and acetylation, histone H3 methylation and/or DNA methylation changes may represent a prerequisite for FS-induced c-Fos and Egr-1 induction in DG neurons and subsequent behavioral responses.

This study shows that FS results in reduced DNA methylation at specific CpGs within c-*Fos* and *Egr-1* gene promoters and untranslated regions in DG neurons. Furthermore, our data show that administration of SAM significantly increases DNA methylation at these c-*Fos* and *Egr-1* gene loci and inhibits c-Fos and Egr-1 induction in DG neurons, impairing consolidation of behavioral responses after FS. Our results indicate that behavioral responses to stress are governed by an intricate balance between methyl donor availability, DNA methylation and DNA demethylation processes.

Results

SAM impairs consolidation of the FS-induced behavioral responses

To investigate the role of methylation-dependent epigenetic mechanisms in stress-induced behavioral responses, we treated rats with the endogenous methyl donor SAM and measured changes in FS-induced behavior (Fig. 1). As endogenous SAM is produced by the liver, we choose to administer the methyl donor systemically. In the initial forced swim session, no (acute) effect of SAM on behavior was found (Fig. 1A). In the retest, however, animals treated with the methyl donor showed significantly less immobility behavior than the vehicle-injected controls (Fig. 1B), indicating that SAM treatment disrupted consolidation of this behavioral response after the initial forced swim session.

SAM attenuates FS-induced c-Fos and Egr-1 induction in DG neurons

Previously, we have shown that the induction of the IEG products c-Fos and Egr-1 in dentate granule neurons is required for the behavioral immobility response observed after FS (5, 11). Therefore, as SAM impaired this behavioral response we determined whether the methyl donor disrupted c-Fos and Egr-1 induction. Rats received a single injection of SAM 30 minutes before FS and were killed 60 minutes after the start of the challenge; a time point when the numbers of c-Fos-positive (c-Fos$^+$) and Egr-1$^+$ DG granule neurons have reached peak levels after stress (5). SAM significantly attenuated the FS-induced increase in c-Fos and completely abolished the rise in Egr-1 among dentate granule neurons (Fig. 2A, B; Fig. S1). These effects occurred specifically among neurons within the dorsal blade of the DG (Fig. S2A, B). The ventral blade neurons were not affected by the stressor (as shown previously (5, 19, 20)) or SAM treatment. The effect of SAM was unique to the

DG as stress-induced c-Fos and Egr-1 expression in the CA1 and CA3 regions of the hippocampus was unaffected by the injected methyl donor (Fig. S3).

FS-induced H3S10p-K14ac formation is not affected by SAM

FS-evoked induction of IEG products c-Fos and Egr-1 in DG granule neurons critically requires H3S10p-K14ac formation (5, 10, 11, 21). Therefore, we investigated whether the inhibitory action of SAM on c-Fos and Egr-1 induction was due to an effect on H3S10p-K14ac formation. For instance, SAM has been shown to increase protein phosphatase activity via methylation (22). Treating rats with SAM before FS however did not affect the formation of H3S10p-K14ac in DG granule neurons (Fig. 3). Furthermore, no effect was seen when immuno-positive neurons in the dorsal and ventral blades were analyzed separately (Fig. S4A). These observations indicate that the methyl donor may attenuate the stress-evoked c-Fos and Egr-1 induction through a mechanism down-stream from H3S10p-K14ac and/or via an alternative, most likely methylation-associated, epigenetic mechanism. Therefore, the role of histone and DNA methylation processes in FS-induced c-Fos and Egr-1 expression was investigated.

FS evokes CpG-specific demethylation at the c-*Fos* and *Egr-1* gene promoters specifically in the DG

Next, we asked whether the effect of FS on c-Fos and Egr-1 involved changes in DNA methylation at specific CpG dinucleotides in the gene promoter and in an area coding for the mRNA's 5' untranslated region (UTR) down-stream from the transcriptional start site (TSS; Fig. S5A, Fig. S6A). In the DG, within Area 2 of the c-*Fos* UTR, CpGs 3 and 4 showed significant hypomethylation after FS, with a trend in the same direction at CpG 5 (Fig. 4). No significant FS-induced changes occurred within Area 1 (Fig. 4). Moreover, in the CA regions, no significant changes in CpG methylation after

stress were observed in Areas 1 and 2 within the c-*Fos* gene promoter and UTR (Fig. S5B) indicating neuroanatomical specificity of stress-induced CpG methylation changes.

FS resulted in significantly reduced DNA methylation at CpGs 5, 11, 13 and 15 in Area A of the *Egr-1* gene promoter in the DG, with near-significant differences at CpGs 7, 8, 14, 16 and 17 (Fig. 5). In Area B, we found a trend of a forced swim effect on the methylation of CpGs 6 and 8 (Fig. 5). In the CA regions, however, CpG methylation in Areas A and B was not affected by the stressor (Fig. S6B).

SAM treatment before forced swim stress increases DNA methylation at specific CpG sites in the c-*Fos* UTR and the *Egr-1* gene promoter in the DG

Given the reduction of DNA methylation observed within the UTR/promoter region of the IEGs in the DG after FS, we examined whether SAM treatment inhibited c-Fos and Egr-1 induction by preventing the stress-evoked CpG demethylation. Our analyses focused on Area 2 in the c-*Fos* UTR (Fig. S5A) and Area A in the *Egr-1* gene promoter (Fig. S6A) as these regions showed the largest stress-induced CpG demethylation.

SAM treatment followed by FS significantly increased methylation of CpGs 1 and 2 in the c-*Fos* UTR (Fig. 6) and CpGs 4-8 and 13 in the *Egr-1* gene promoter (Fig. 7). CpG methylation did not increase in the SAM-injected animals killed under baseline conditions, indicating that increased availability of the methyl donor, in the absence of a stressful challenge, is insufficient to increase CpG methylation in these DG neurons. Furthermore, except for an increase in CpG 1 methylation in the baseline group and a decrease in CpG 1 and 2 methylation in the stressed group in c-Fos Area 2, SAM administration did not change CpG methylation at either IEG gene promoter/UTR in the CA regions (Fig. S7).

Although we observed a significant main effect of stress on DNA methylation levels, post-hoc analyses did not identify a significant effect of FS on DNA methylation levels at individual CpGs in the vehicle-treated stressed rats compared with vehicle-treated baseline controls (Fig. 6, 7). Given the

apparent stress sensitivity of CpG methylation levels in the UTR/promoters of IEGs it is likely that the psychological stress associated with the injection has masked the effect of FS in the vehicle-treated groups.

As SAM is the universal methyl donor, we checked whether FS and SAM would affect histone methylation processes within the IEG gene loci under study. We studied histone H3 methylation changes known to be involved in either gene activity (H3K4me3; histone H3 tri-methylated at lysine-4)) or gene suppression (H3K9me3, H3K27me3). Figure S8 shows that SAM and FS did not alter these methylated histone marks within the *c-Fos* UTR and the *Egr-1* gene promoter.

FS increases Dnmt3a mRNA expression in the DG

As FS in conjunction with SAM treatment resulted in increased DNA methylation at specific CpG sites in the c-*Fos* and *Egr-1* genes, we investigated the effect of FS on mRNA expression of several members of the *Dnmt* family, as possible mediators of the observed increase in DNA methylation, as well as mRNA expression of *Tet1*, a key enzyme in DNA demethylation. In the DG, *Dnmt3a* expression was significantly increased immediately after the 15 min FS session (Fig. 8A) whereas no forced swim effect on *Dnmt3a* expression was found in the CA regions of the hippocampus (Fig. 8B). The expression of *Dnmt3b*, *Dnmt1* and *Tet1* mRNA remained unchanged after FS in both the DG and CA regions (Fig. S9).

Increased association of Dnmt3a with the *c-Fos* UTR and *Egr-1* gene promoter after FS

To investigate whether the increased *Dnmt3a* mRNA results in increased association of this Dnmt with the *c-Fos* UTR and *Egr-1* gene promoter regions, we conducted ChIP assays for Dnmt3a. We also conducted Dnmt3b and Tet1 ChIP assays to check whether FS might induce enrolment of (de-)methylating proteins to the chromatin independent of increased expression. We found that FS

resulted in a significantly increased association of Dnmt3a, but not Dnmt3b or Tet1, with these regions in the IEG genes (Fig. 9). Association of Dnmt3b was significantly reduced at the *Egr1* promoter after stress, indicating that there is a locus-specific decrease in Dnmt3b binding in the absence of gene expression changes (Fig. 9B). Thus, increased Dnmt3a expression and gene association after FS together with the elevated levels of SAM may underlie the increased CpG methylation at the c-*Fos* UTR and *Egr-1* gene promoter in the DG resulting in suppressed c-Fos and Egr-1 gene expression and impaired behavioral responses to the stressor.

Discussion

A sole traumatic event has long-term implications for future behavioral responses to similar incidents. Here we show that the DNA methylation status at the c-*Fos* and *Egr-1* gene promoters, specifically in sparsely activated DG neurons, plays a crucial role in the consolidation of immobility behavior after FS. The stressful event evoked the demethylation of distinct CpGs within the promoter and UTR of these IEGS. Conversely, elevation of methyl donor availability led, in the stressed animals, to markedly elevated CpG methylation, inhibition of IEG expression and impaired immobility behavior. The observed changes in DNA methylation may be due to the increased *Dnmt3a* expression and the increased association of this Dnmt with the IEG loci in these DG neurons.

FS evoked CpG-specific demethylation events in the DG but not in the hippocampal CA region. Region-specific active DNA demethylation has been shown to play a role in activity-induced gene expression in DG granule neurons, likely mediated by Tet1 and/or Gadd45b (23-25). Furthermore, DNA demethylation in the DG also occurred after voluntary running (24). Thus, DG neurons have been found to be rather susceptible to DNA methylation changes in response to environmental stimuli. The gene expression changes in the DG after such stimuli are known to occur in sparsely distributed neurons (5, 10, 11) suggesting that the observed DNA demethylation events are also occurring in these neurons.

The methyl donor SAM had a strong effect on FS-induced gene expression and behavioral responses. The disruption of the behavioral immobility response by SAM corresponds with earlier observations made in both rats and mice (18). Until now, the underlying molecular mechanism of action of SAM on this behavioral response was unknown. SAM had no effect on baseline c-Fos and Egr-1 expression but strongly inhibited the FS-evoked IEG responses specifically in DG granule neurons. No effect of

the methyl donor was observed on IEGs in CA1 and CA3 regions of the hippocampus. Furthermore, there was no effect of SAM and FS on histone methylation at these genes. Previously, we have shown that FS-induced c-Fos and Egr-1 in DG neurons are critically involved in the consolidation of the behavioral immobility response (5). The neuroanatomically selective effect of SAM further underscores the importance of IEG expression in DG neurons for this stress-induced behavioral response. Furthermore, the induction of these IEGs in DG neurons requires the formation of the dual histone mark H3S10p-K14ac within the promoter regions of these genes. The formation of this epigenetic mark is the result of concomitant GR and NMDA-ERK-MSK1-Elk-1 signaling in these DG neurons (5). Clearly, SAM had no effect on the formation of this dual histone mark indicating that the methyl donor did not produce its effects on gene expression and behavior through interference with these signaling pathways. Therefore, the methyl donor appears to act via a methylation/demethylation mechanism down-stream of the dual histone modifications.

In our studies, SAM affected DNA methylation only under stress conditions. Administration of SAM before FS resulted in significant increases in DNA methylation within areas of the c-*Fos* 5'-UTR and *Egr-1* promoter in the DG that had previously shown demethylation after the stressor only. In vehicle-injected rats, FS failed to result in significant demethylation possibly due to (restraint) stress associated with the injection underlining that DNA methylation status of these CpGs is highly stress-sensitive. As SAM is an endogenous methyl donor synthesized by S-adenosylmethionine synthetase mainly in the liver, the observation that this methyl donor markedly affects stress-induced gene expression and behavioral responses has greater physiological implications. We show that the impact of stressful events like FS on gene expression and behavior may depend on the cellular concentration of SAM. Presently, little is known of the regulation of S-adenosylmethionine synthetase activity and the control of SAM uptake in the brain. In yeast, a mechanism for sensing SAM levels was revealed which would determine metabolic processes underlying growth (22).

Possibly, the mammalian brain also has a mechanism for monitoring SAM levels that determines the neuronal response to environmental stimuli.

The exact mechanism through which FS in the presence of elevated SAM levels inhibit IEG expression still needs to be clarified. Within the c-*Fos* gene, SAM- and stress-evoked CpG methylation changes occurred mainly within Area 2, which is located down-stream from the TSS in a region that codes for the 5' UTR of the mRNA molecule. RNA-polymerase II and associated factors assemble upstream of the TSS and produce short RNA fragments; however, additional mechanisms are required before full-length transcripts can be produced. This poised state of gene transcription allows a rapid induction of c-Fos in response to stimuli (26). The CpGs within Area 2 of the c-*Fos* gene reside within the window of elongation termination, which is between +30 and +60 bps after the TSS (27). Therefore, as DNA methylation can prevent transcriptional elongation (28), the SAM and FS-induced CpG methylation increases may result in premature termination of the c-*Fos* transcript in the DG neurons. Area A within the *Egr-1* promoter is approximately 500 bps upstream from the TSS. Increased DNA methylation in this region could influence transcription factor binding and disrupt chromatin remodeling and/or assembly of transcriptional machinery. For instance, *in silico* analysis of transcription factor binding sites presented Sp1 (specificity protein 1) and Klf9 (Krüppel-like factor 9) sites within the DNA sequence of Area A. The *Klf9* gene contains glucocorticoid response elements (GREs) and expression is induced in response to elevated corticosterone levels (29), which are known to occur after FS (30). Thus, the SAM and FS-induced increases in CpG methylation in this region of the *Egr-1* gene may have disrupted Klf9-mediated (and possibly Sp1-mediated) transcriptional activation but confirmation of this postulate requires further investigation.

FS resulted in an increased expression of the *de novo* DNA methyltransferase *Dnmt3a* (but not *Dnmt3b*, *Dnmt1* and *Tet1*) specifically in the DG. This enhanced expression after stress, in the presence of elevated SAM levels, may be responsible for the increased CpG methylation in the c-*Fos*

UTR and *Egr-1* gene promoter resulting in inhibition of gene expression and impaired behavioral responses. The increased recruitment of Dnmt3a at these IEG loci after FS supports this notion; however, in the context of normal SAM levels this observation appears to be contradictory as FS results in DNA demethylation at the IEG loci and increased expression of c-Fos and Egr-1. Observations made *in vitro* may explain this apparent paradox. Dnmt3a has been shown to function as a DNA demethylase under conditions of elevated Ca^{2+} levels, whereas the methyltransferase activity was reinstated after raising SAM levels (31-33). Induction of IEGs in DG neurons *in vivo* requires the opening of NMDA receptors allowing a sustained rise in intracellular Ca^{2+} levels (11). In view of the findings of Chen et al. (33), it may be expected that the risen Ca^{2+} levels favor the DNA demethylase activity of the recruited Dnmt3a enzyme resulting in the demethylation at the IEG loci that we observed. When SAM levels were elevated in our study apparently the enzyme activity of the recruited Dnmt3a shifted to a methyltransferase activity resulting in DNA methylation of the IEG loci. Together, these data suggest that the DNA methylation status is not only governed by the recruitment (and expression levels) of DNA methylating/demethylating enzymes but also by the concentration of SAM and other physiological factors (e.g. Ca^{2+}).

The mechanisms controlling the increased association of Dnmt3a with the c-*Fos* and *Egr-1* gene loci after FS are unknown, but may involve changes in the chromatin structure (e.g. through local H3S10p-K14ac formation (see above)) as well as post-translational modifications of Dnmt3a that regulate its affinity for binding partners (34, 35). Previous work has shown that Dnmts play an important role in hippocampus-dependent learning (15, 36) Furthermore, *Dnmt3a* expression increases in the hippocampus after contextual fear conditioning (14) and is upregulated in the DG after electroconvulsive shock (24), highlighting the importance of this *de novo* methyltransferase in activity-induced neuronal function. The possibility that Dnmt3a may function as a DNA demethylase in FS-activated neurons suggests additional layers of complexity to stressor-induced epigenomic regulation which should be explored.

Our work shows that, after FS, not only is *Dnmt3a* expression increased in the DG but so is its association with IEG loci; nevertheless, the levels of SAM determine the impact on IEG induction and the consolidation of the behavioral immobility response. Presently, it is unknown to what extent SAM levels determine responses in other hippocampus-dependent behavioral models like Morris water maze learning and contextual fear condition. Our results indicate that the neuronal concentration of SAM is a key factor in the molecular and behavioral responses evoked by environmental challenges. This notion is supported by work *in vitro* which demonstrates that inhibition of Dnmts disrupts hippocampal neuron function, but this is rescuable by elevating SAM levels (37), indicating that a tightly controlled balance between Dnmt activity and SAM is important for normal hippocampal neuron function. Accordingly, it seems that a tight control of SAM synthesis (and Dnmt function) is of pivotal physiological importance.

In summary, the induction of IEGs in DG granule neurons is highly complex. Neuronal activation due to stressful stimuli is regulated by NMDA, GABA-A and glucocorticoid receptors, ERK MAPK signaling, H3S10p-K14ac formation (5, 11, 21), and, as shown in the present study, by distinct CpG methylation events. It appears that IEG induction is checked by multi-level control mechanisms whereby the CpG methylation status plays a go/no-go role. The control of IEG induction in DG neurons is reflected in the (long-term) consolidation of the behavioral response after FS. The stressful challenge also resulted in increased expression of the *de novo* methyltransferase *Dnmt3a*, which may act as a DNA demethylase in the context of normal SAM levels and elevated Ca^{2+} in activated DG neurons. In contrast, if SAM levels were elevated, stress led to an increased methylation of CpGs within the gene/gene promoter of the IEGs resulting in suppressed gene expression and impaired behavioral responses. Thus, our study shows that CpG methylation status is an important controller of IEG expression in DG neurons. Moreover, we revealed that the levels of available SAM, possibly in conjunction with Dnmt3a expression and action, are a determining factor

in the responsiveness of DG neurons to environmental stimuli with significant consequences for the organism in terms of gene expression and behavior.

Materials and Methods

Animals and Drug Treatment. Male Wistar rats (150-175 g) were purchased form Harlan and group housed. Rats were forced to swim for 15min in 25 °C water or left undisturbed (refs 11, 19 in MGM). Some animals received pretreatment with a drug or the vehicle 30min before FS. Rats were killed at the indicated times (see legends) after FS or were kept until 24h later to undergo another FS test (retest) for 5min. Behavior was scored every 10 s during the first 5 min of the test and retest. The drug used was SAM (100 mg/kg body weight) to raise levels of the endogenous methyl donor. For more information, see *SI Materials and Methods*.

Tissue preparation. For immunohistochemistry rats were perfused with saline and 4% paraformaldehyde and inhibitors. Brains were cut into 50-μm coronal sections and kept at 4 °C. For other studies, after decapitation the entire hippocampus was dissected or the DG and CA regions were micro-dissected from the dorsal hippocampus in 1-mm coronal brain slices. Tissues were snap frozen in liquid N_2 and stored at -80 °C. For more information, see *SI Materials and Methods*.

Immunohistochemistry. Immunohistochemistry was conducted using published methods (5). For more information, see *SI Materials and Methods*.

Bisulfite pyrosequencing. Genomic DNA from DG and CA regions was subjected to bisulfite conversion and pyrosequenced as described in the *SI Materials and Methods*.

ChIP, RNA analysis and qPCR. ChIP and RNA extraction was performed using published methods (7, 38, 39). For a complete description, see *SI Materials and Methods*.

Statistical analysis. Data were analysed by ANOVA, Student's t-test and appropriate post-hoc tests. For more information, see *SI Materials and Methods*.

Acknowledgments

This research was supported by grants from the Biotechnology and Biological Sciences Research Council (BBSRC), Medical Research Council (MRC) and the British Pharmacological Society.

References

1. De Kloet ER, Oitzl MS, & Joels M (1999) Stress and cognition: are corticosteroids good or bad guys? *Trends Neurosci.* 22(10):422-426.
2. Caamano CA, Morano MI, & Akil H (2001) Corticosteroid receptors: a dynamic interplay between protein folding and homeostatic control. Possible implications in psychiatric disorders. *Psychopharmacol.Bull.* 35(1):6-23.
3. Reul JMHM (2014) Making memories of stressful events: a journey along epigenetic, gene transcription, and signaling pathways. *Front Psychiatry* 5(:5.
4. De Kloet ER, De Kock S, Schild V, & Veldhuis HD (1988) Antiglucocorticoid RU 38486 attenuates retention of a behaviour and disinhibits the hypothalamic-pituitary adrenal axis at different brain sites. *Neuroendocrinology* 47(:109-115.
5. Gutierrez-Mecinas M et al. (2011) Long-lasting behavioral responses to stress involve a direct interaction of glucocorticoid receptors with ERK1/2-MSK1-Elk-1 signaling. *Proc.Natl.Acad.Sci.U.S.A* 108(33):13806-13811.
6. Chwang WB, O'Riordan KJ, Levenson JM, & Sweatt JD (2006) ERK/MAPK regulates hippocampal histone phosphorylation following contextual fear conditioning. *Learn.Mem.* 13(3):322-328.
7. Carter SD, Mifsud KR, & Reul JMHM (2015) Distinct epigenetic and gene expression changes in rat hippocampal neurons after Morris water maze training. *Front Behav.Neurosci* 9(:156.
8. Oitzl MS, De Kloet ER, Joels M, Schmid W, & Cole TJ (1997) Spatial learning deficits in mice with a targeted glucocorticoid receptor gene disruption. *Eur.J.Neurosci.* 9(11):2284-2296.
9. Jones MW et al. (2001) A requirement for the immediate early gene Zif268 in the expression of late LTP and long-term memories. *Nat.Neurosci.* 4(3):289-296.

10. Bilang-Bleuel A et al. (2005) Psychological stress increases histone H3 phosphorylation in adult dentate gyrus granule neurons: involvement in a glucocorticoid receptor-dependent behavioural response. *Eur.J.Neurosci.* 22(7):1691-1700.

11. Chandramohan Y, Droste SK, Arthur JS, & Reul JMHM (2008) The forced swimming-induced behavioural immobility response involves histone H3 phospho-acetylation and c-Fos induction in dentate gyrus granule neurons via activation of the N-methyl-D-aspartate/extracellular signal-regulated kinase/mitogen- and stress-activated kinase signalling pathway. *Eur.J.Neurosci.* 27(10):2701-2713.

12. Liu X et al. (2012) Optogenetic stimulation of a hippocampal engram activates fear memory recall. *Nature* 484(7394):381-385.

13. Hunter RG, McCarthy KJ, Milne TA, Pfaff DW, & McEwen BS (2009) Regulation of hippocampal H3 histone methylation by acute and chronic stress. *Proc.Natl.Acad.Sci.U.S.A*.

14. Miller CA & Sweatt JD (2007) Covalent modification of DNA regulates memory formation. *Neuron* 53(6):857-869.

15. Feng J et al. (2010) Dnmt1 and Dnmt3a maintain DNA methylation and regulate synaptic function in adult forebrain neurons. *Nat.Neurosci.*

16. Gupta S et al. (2010) Histone methylation regulates memory formation. *J.Neurosci.* 30(10):3589-3599.

17. Fleischmann A et al. (2003) Impaired long-term memory and NR2A-type NMDA receptor-dependent synaptic plasticity in mice lacking c-Fos in the CNS. *J.Neurosci.* 23(27):9116-9122.

18. Czyrak A, Rogoz Z, Skuza G, Zajaczkowski W, & Maj J (1992) Antidepressant activity of S-adenosyl-L-methionine in mice and rats. *J.Basic Clin.Physiol Pharmacol.* 3(1):1-17.

19. Chandramohan Y, Droste SK, & Reul JMHM (2007) Novelty stress induces phospho-acetylation of histone H3 in rat dentate gyrus granule neurons through coincident signalling via the N-

methyl-d-aspartate receptor and the glucocorticoid receptor: relevance for c-fos induction. *J.Neurochem.* 101(3):815-828.

20. Collins A et al. (2009) Exercise improves cognitive responses to psychological stress through enhancement of epigenetic mechanisms and gene expression in the dentate gyrus. *PLoS.One* 4(:e4330.
21. Papadopoulos A et al. (2010) GABAergic control of stress-responsive epigenetic and gene expression mechanisms in the dentate gyrus. *Eur.Neuropsychopharmacol.* 21(:316-324.
22. Sutter BM, Wu X, Laxman S, & Tu BP (2013) Methionine inhibits autophagy and promotes growth by inducing the SAM-responsive methylation of PP2A. *Cell* 154(2):403-415.
23. Ma DK et al. (2009) Neuronal activity-induced Gadd45b promotes epigenetic DNA demethylation and adult neurogenesis. *Science* 323(5917):1074-1077.
24. Guo JU et al. (2011) Neuronal activity modifies the DNA methylation landscape in the adult brain. *Nat.Neurosci.*
25. Guo JU, Su Y, Zhong C, Ming GL, & Song H (2011) Hydroxylation of 5-methylcytosine by TET1 promotes active DNA demethylation in the adult brain. *Cell* 145(3):423-434.
26. Fivaz J, Bassi MC, Pinaud S, & Mirkovitch J (2000) RNA polymerase II promoter-proximal pausing upregulates c-fos gene expression. *Gene* 255(2):185-194.
27. Levine M (2011) Paused RNA polymerase II as a developmental checkpoint. *Cell* 145(4):502-511.
28. Rountree MR & Selker EU (1997) DNA methylation inhibits elongation but not initiation of transcription in Neurospora crassa. *Genes Dev.* 11(18):2383-2395.
29. Bagamasbad P et al. (2012) Molecular basis for glucocorticoid induction of the Kruppel-like factor 9 gene in hippocampal neurons. *Endocrinology* 153(11):5334-5345.
30. Bilang-Bleuel A, Rech J, Holsboer F, & Reul JMHM (2002) Forced swimming evokes a biphasic response in CREB phosphorylation in extrahypothalamic limbic and neocortical brain structures. *Eur.J.Neurosci.* 15(:1048-1060.

31. Metivier R et al. (2008) Cyclical DNA methylation of a transcriptionally active promoter. *Nature.* 452(7183):45-50.

32. Chen CC, Wang KY, & Shen CK (2012) The mammalian de novo DNA methyltransferases DNMT3A and DNMT3B are also DNA 5-hydroxymethylcytosine dehydroxymethylases. *J.Biol.Chem.* 287(40):33116-33121.

33. Chen CC, Wang KY, & Shen CK (2013) DNA 5-methylcytosine demethylation activities of the mammalian DNA methyltransferases. *J.Biol.Chem.* 288(13):9084-9091.

34. Ling Y et al. (2004) Modification of de novo DNA methyltransferase 3a (Dnmt3a) by SUMO-1 modulates its interaction with histone deacetylases (HDACs) and its capacity to repress transcription. *Nucleic Acids Res.* 32(2):598-610.

35. Deplus R et al. (2014) Citrullination of DNMT3A by PADI4 regulates its stability and controls DNA methylation. *Nucleic Acids Res.* 42(13):8285-8296.

36. Feng J, Chang H, Li E, & Fan G (2005) Dynamic expression of de novo DNA methyltransferases Dnmt3a and Dnmt3b in the central nervous system. *J.Neurosci Res.* 79(6):734-746.

37. Nelson ED, Kavalali ET, & Monteggia LM (2008) Activity-dependent suppression of miniature neurotransmission through the regulation of DNA methylation. *J.Neurosci* 28(2):395-406.

38. Stock JK et al. (2007) Ring1-mediated ubiquitination of H2A restrains poised RNA polymerase II at bivalent genes in mouse ES cells. *Nat.Cell Biol.* 9(12):1428-1435.

39. Chomczynski P & Sacchi N (1987) Single-step method of RNA isolation by acid guanidinium thiocyanate-phenol-chloroform extraction. *Anal.Biochem.* 162(1):156-159.

40. Paxinos G & Watson C. The rat brain in sterotaxic coordinates. 2nd Edition. 1986. San Diego, California, Academic Press Inc.

41. Demir O & Kurnaz IA (2008) Wildtype Elk-1, but not a SUMOylation mutant, represses egr-1 expression in SH-SY5Y neuroblastomas. *Neurosci Lett.* 437(1):20-24.

42. Leyva-Illades D, Cherla RP, Galindo CL, Chopra AK, & Tesh VL (2010) Global transcriptional response of macrophage-like THP-1 cells to Shiga toxin type 1. *Infect.Immun.* 78(6):2454-2465.

43. Kent WJ (2002) BLAT--the BLAST-like alignment tool. *Genome Res.* 12(4):656-664.

44. Gibbs RA et al. (2004) Genome sequence of the Brown Norway rat yields insights into mammalian evolution. *Nature* 428(6982):493-521.

45. Egelhofer TA et al. (2011) An assessment of histone-modification antibody quality. *Nat.Struct.Mol.Biol.* 18(1):91-93.

46. Pfaffl MW (2001) A new mathematical model for relative quantification in real-time RT-PCR. *Nucleic Acids Res.* 29(9):e45.

Figure legends

Figure 1. The effect of SAM on FS-induced behaviour. Rats were given one injection of vehicle or SAM (100 mg/kg, s.c.) 30 min before FS (15 min, 25°C) and 24 hours later were forced to swim again under the same conditions. The graphs show the climbing, swimming and immobility behaviour scored in 10 s bins during the first 5 min of the initial test (A) and retest (B). Data are shown as the mean behavioral score (mean ± SEM, n = 8-9). *, $p < 0.05$ compared with the respective vehicle-treated group; $^{\&}$, $p = 0.072$ compared with the respective vehicle-treated group. For more information on statistical analyses in Figures 1-7, see Supplemental Statistics Information.

Figure 2. The effect of SAM on FS-evoked c-Fos and Egr-1 induction in the DG. Rats were given one injection of vehicle or SAM (100 mg/kg, s.c.) 30 min before FS (15 min, 25°C) and killed 60 min after the start of the challenge (FS60). The baseline (BL) groups were killed 90 min after injection. The graphs show the number of c-Fos$^+$ and Egr-1$^+$ neurons in the whole DG within a 50 µm section (A and B respectively). Data are shown as the average number of c-Fos$^+$ or Egr-1$^+$ neurons from three, 50 µm-thick coronal brain slices per animal (mean ± SEM, n = 5-6). *, $p < 0.05$ compared with the respective BL group; $^{\$}$, $p < 0.05$ compared with the respective vehicle/FS60 group.

Figure 3. The effect of SAM on H3S10p-K14ac formation in the DG after FS. Rats were given one injection of vehicle or SAM (100 mg/kg, s.c.) 30 min before FS (15 min, 25°C) and killed at FS60. The BL groups were killed 90 min after the injection. The graphs show the number of H3S10p-K14ac$^+$ neurons in the DG. Data are shown as an average number of H3S10p-K14ac$^+$ neurons from three, 50 µm-thick coronal brain slices per animal (mean ± SEM, n = 4-6). *, $p < 0.05$ compared with the respective BL group; $^{\#}$, $p < 0.05$ compared with the respective ventral blade group

Figure 4. FS-induced CpG-specific DNA methylation changes in the c-*Fos* promoter region. Rats were killed immediately (BL group) or subjected to FS (15 min, 25°C) and killed at FS60. The location of CpGs within Areas 1 and 2 with respect to the rat c-*Fos* gene are shown in Fig. S5. The graphs show DNA methylation changes at CpGs in Area 1 and Area 2 in the DG (C). Data are shown as percentage methylation (mean ± SEM, n = 3-6). *, $p < 0.05$; &, $p < 0.1$, compared with the respective BL group

Figure 5. FS-induced CpG-specific DNA methylation changes in the *Egr-1* promoter region. Rats were killed immediately (BL group) or subjected to FS (15 min, 25°C) and killed at FS60. The location of CpGs within Areas A and B with respect to the rat *Egr-1* gene are shown in Fig. S6. The graphs show DNA methylation changes at CpGs in Area A and Area B in the DG. Data are shown as percentage methylation (mean ± SEM, n = 5-6). *, $p < 0.05$; &, $p < 0.1$, compared with the respective BL group

Figure 6. The effect of SAM treatment on FS-induced DNA methylation changes at CpGs within the c-*Fos* UTR in the DG. Rats were given one injection of vehicle or SAM (100 mg/kg, s.c.) 30 min before FS (15 min, 25°C) and killed at FS60. The BL groups were killed 90 min after the injection. The graph shows methylation of CpGs in Area 2 of the c-*Fos* UTR in the DG. Data are shown as percentage methylation (mean ± SEM, n = 4-6). *, $p < 0.05$ compared with the respective vehicle/FS60 group; $^{\$}$, $p < 0.05$ compared with the respective SAM/BL group; $^{+}$, $p = 0.076$ compared with the respective SAM/BL group; $^{\&}$, $p = 0.076$ compared with the respective vehicle/FS60 group

Figure 7. The effect of SAM treatment on FS-induced DNA methylation changes at CpGs within the *Egr-1* gene promoter in the DG. Rats were given one injection of vehicle or SAM (100 mg/kg, s.c.) 30 min before FS (15 min, 25°C) and killed at FS60. The BL groups were killed 90 min after the injection. The location of CpGs within Area A with respect to the *Egr-1* gene is shown in Fig. S6. The graph shows methylation of CpGs in Area A of the *Egr-1* gene promoter in the DG. Data are shown as percentage methylation (mean ± SEM, n = 4-6). *, $p < 0.05$ compared with the respective vehicle/FS60 group; $^{\$}$, $p < 0.05$ compared with the respective SAM/BL group.

Figure 8. Effect of FS on *Dnmt3a* mRNA expression in the DG and CA regions of the hippocampus. Rats were killed immediately (BL group) or subjected to FS (15 min, 25°C) and killed immediately (FS15), 30 min (FS30), 60 min (FS60) or 180 min (FS180) after the start of the challenge. The graphs show *Dnmt3a* mRNA expression in the DG (A) and the CA regions (B) of the hippocampus. Data are shown as relative mRNA copy number standardised to the expression of the house keeping genes *Hprt1* and *Ywhaz* (mean ± SEM, n = 8-9). Statistical analysis: one-way ANOVA; (A) $F_{(5,38)} = 3.0$, $p < 0.05$. (B) $F_{(5,39)} = 0.97$, $p = 0.43$. Dunnett's post-hoc test: *, $p < 0.05$ compared with the BL group.

Figure 9. Association of Dnmt3a, Dnmt1 and Tet1 with c-Fos and Egr-1 gene loci after FS. Rats were killed under baseline conditions or at 60 min after the start of a 15min FS session (FS60). ChIP for Dnmt3a, Dnmt3b and Tet1 was conducted on hippocampus tissue followed by qPCR for the c-Fos (A) and Egr-1 (B) loci studied for DNA methylation changes after SAM and FS. Data are expressed as the enrichment of the respective enzymes at the loci at FS60 relative to that in the baseline situation (mean ± SEM, n = 4). *, $P < 0.01$, Student's t-test

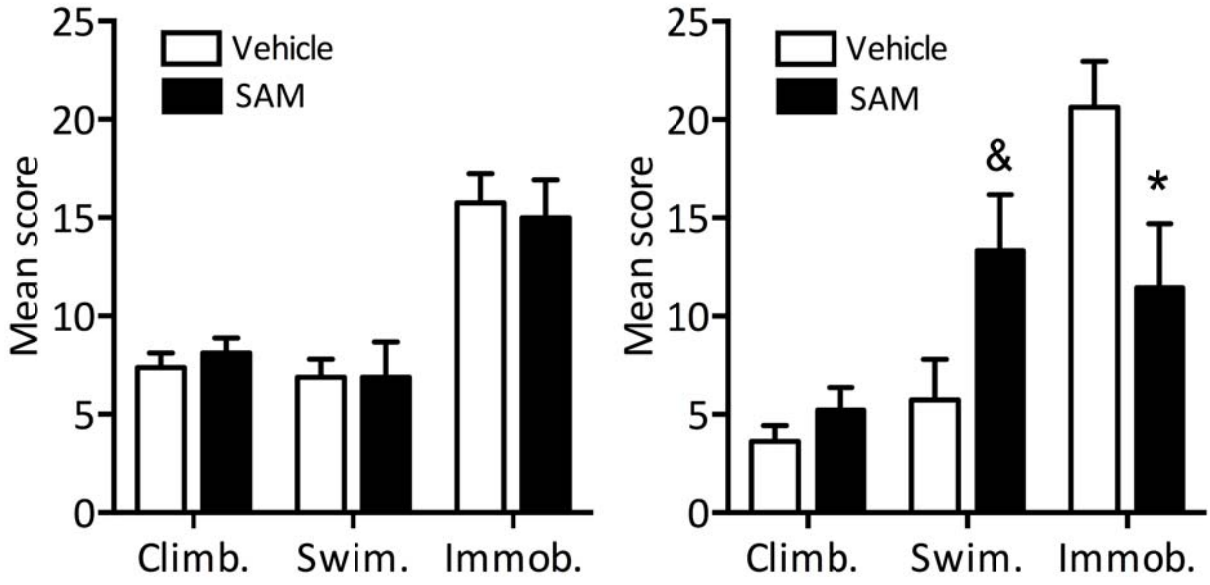

Figure 1

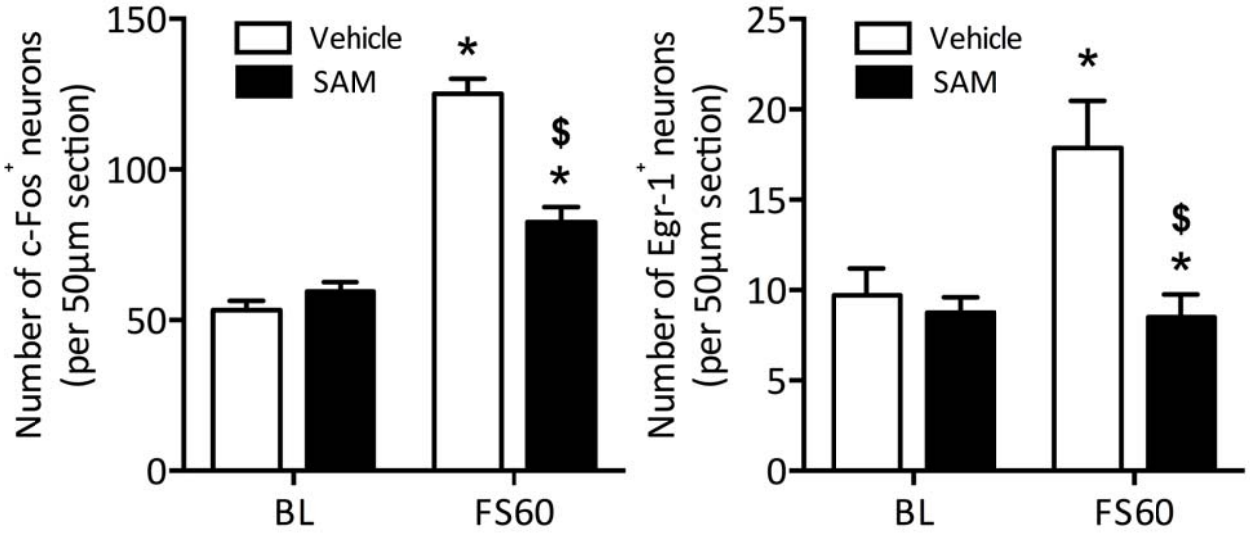
Number of c-Fos+ neurons (per 50µm section)
150
100
50
0
Vehicle
SAM
*
* $
BL
FS60
Number of Egr-1+ neurons (per 50µm section)
25
20
15
10
5
0
Vehicle
SAM
*
* $
BL
FS60

Figure 2

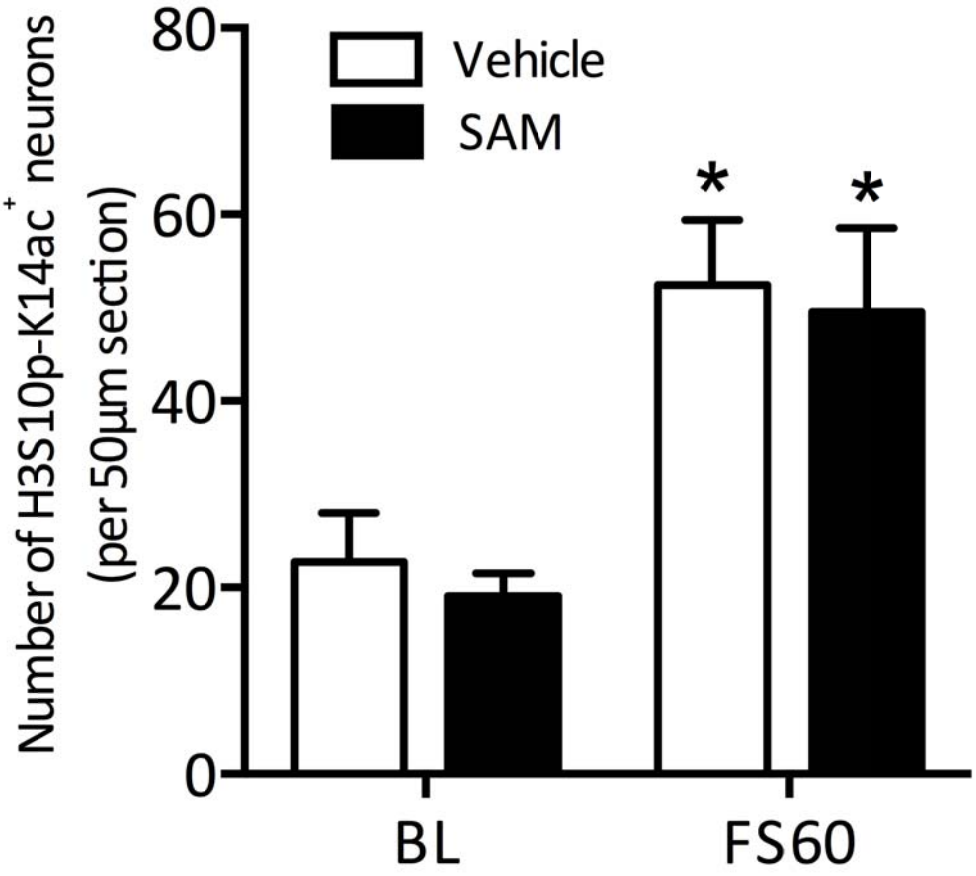
Number of H3S10p-K14ac+ neurons
(per 50µm section)
80
60
40
20
0
Vehicle
SAM
*
*
BL
FS60

Figure 3

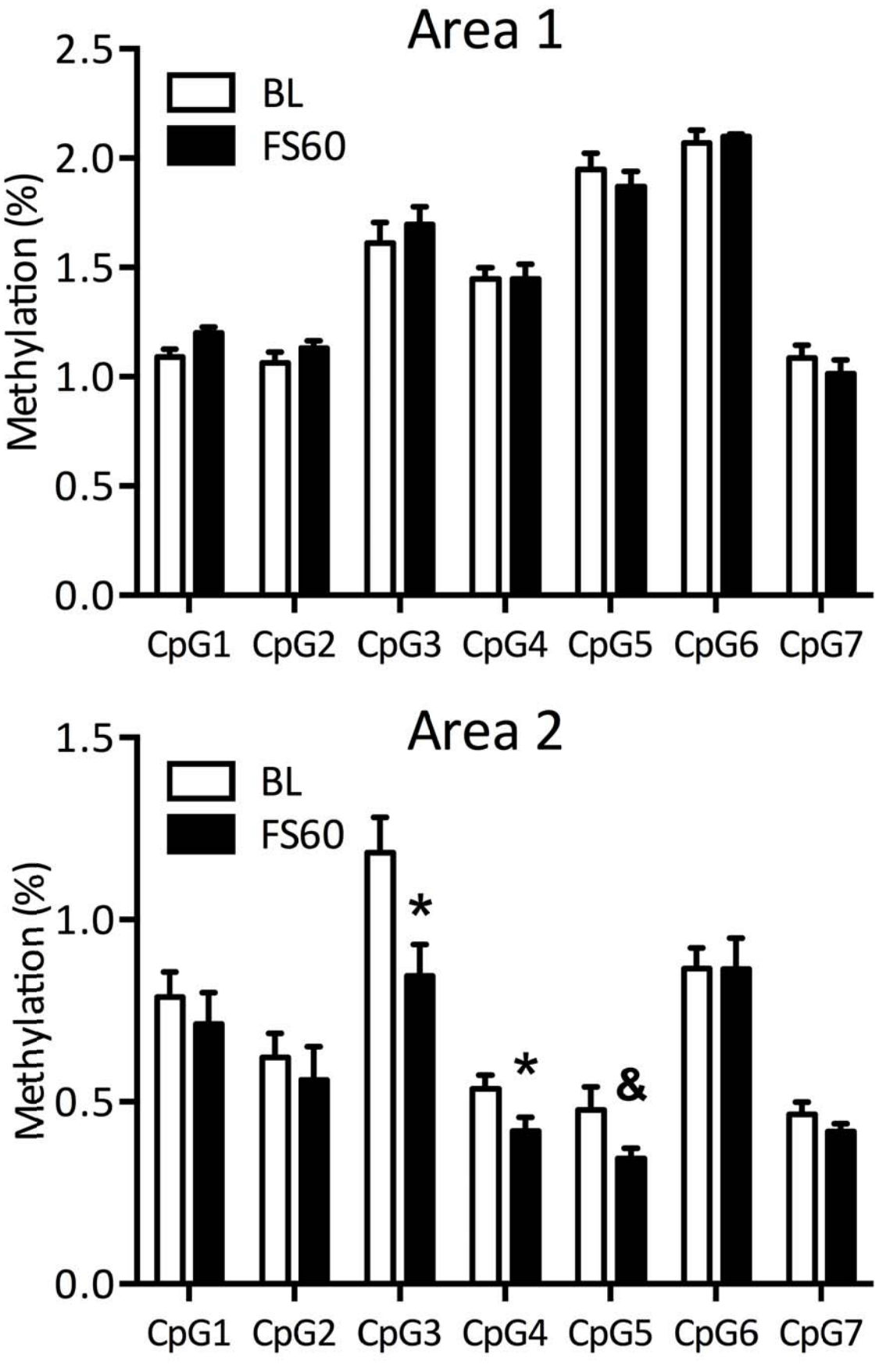
Area 1
BL
FS60
Methylation (%)
2.5
2.0
1.5
1.0
0.5
0.0
CpG1
CpG2
CpG3
CpG4
CpG5
CpG6
CpG7
Area 2
BL
FS60
Methylation (%)
1.5
1.0
0.5
0.0
*
*
&
CpG1
CpG2
CpG3
CpG4
CpG5
CpG6
CpG7

Figure 4

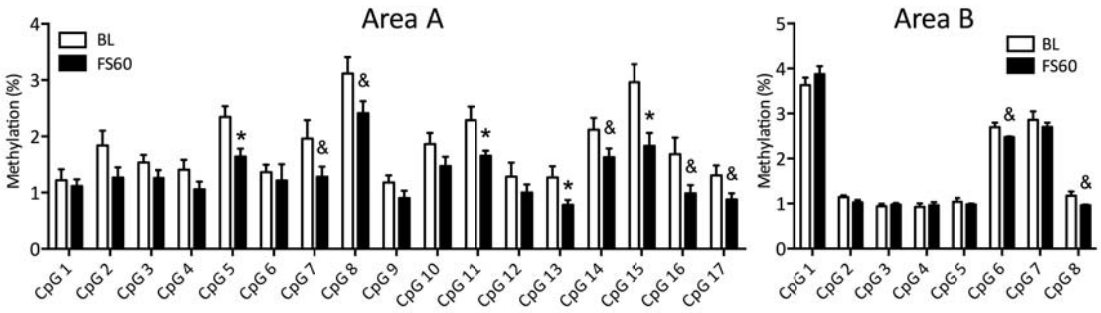
Area A
BL
FS60
Methylation (%)
0
1
2
3
4
CpG 1
CpG 2
CpG 3
CpG 4
CpG 5
CpG 6
CpG 7
CpG 8
CpG 9
CpG 10
CpG 11
CpG 12
CpG 13
CpG 14
CpG 15
CpG 16
CpG 17
Area B
BL
FS60
Methylation (%)
0
1
2
3
4
5
CpG 1
CpG 2
CpG 3
CpG 4
CpG 5
CpG 6
CpG 7
CpG 8

Figure 5

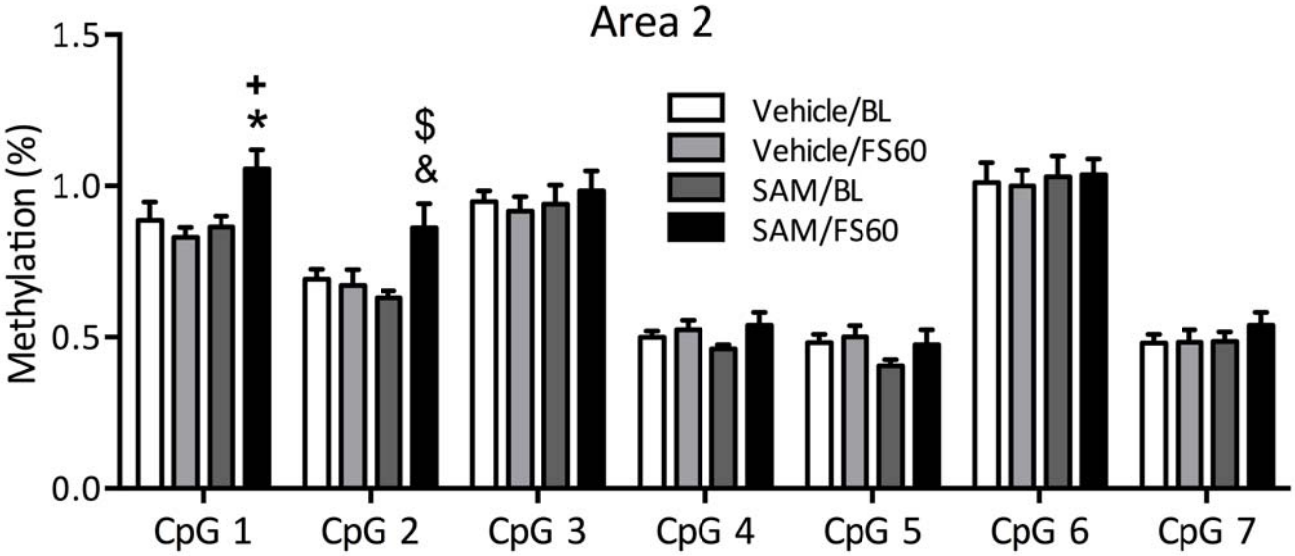
Area 2
Methylation (%)
1.5
1.0
0.5
0.0
+
*
$
&
Vehicle/BL
Vehicle/FS60
SAM/BL
SAM/FS60
CpG 1
CpG 2
CpG 3
CpG 4
CpG 5
CpG 6
CpG 7

Figure 6

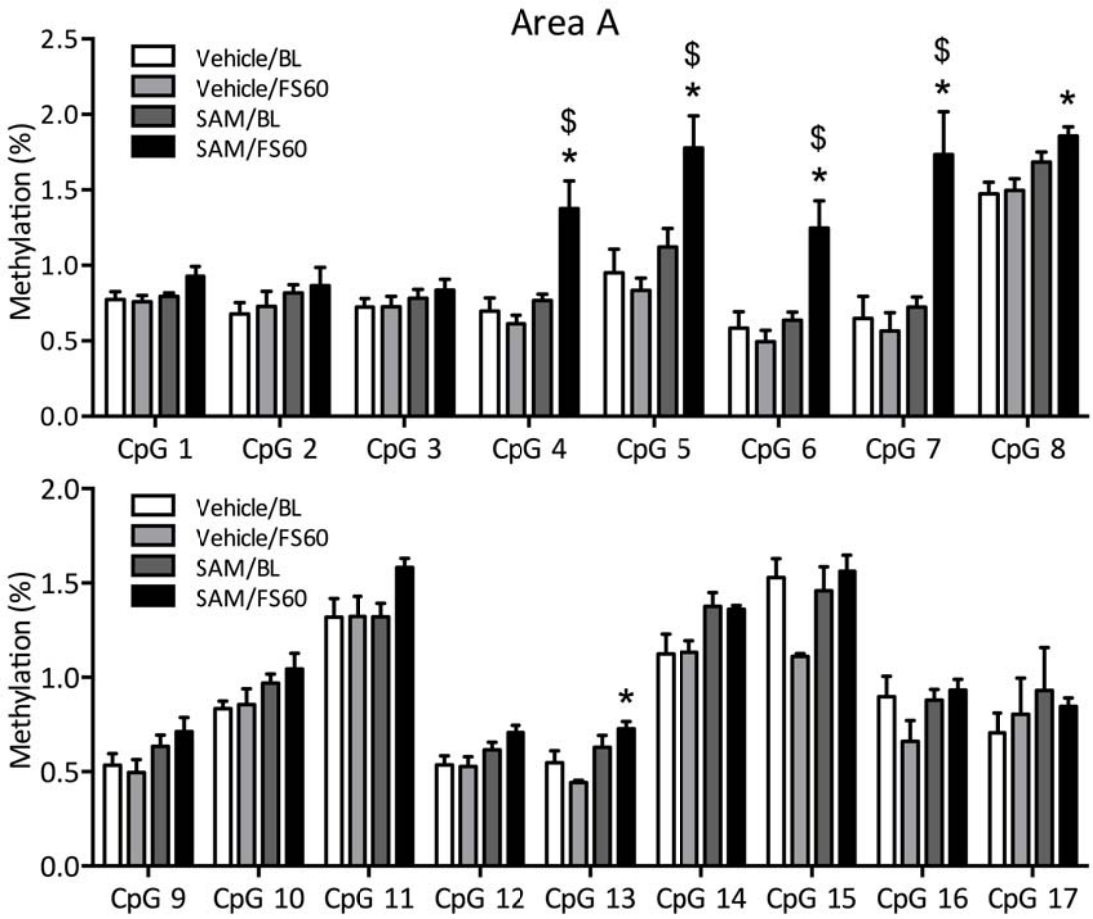
Area A
Vehicle/BL
Vehicle/FS60
SAM/BL
SAM/FS60
Methylation (%)
2.5
2.0
1.5
1.0
0.5
0.0
$
*
CpG 1
CpG 2
CpG 3
CpG 4
CpG 5
CpG 6
CpG 7
CpG 8
CpG 9
CpG 10
CpG 11
CpG 12
CpG 13
CpG 14
CpG 15
CpG 16
CpG 17

Figure 7

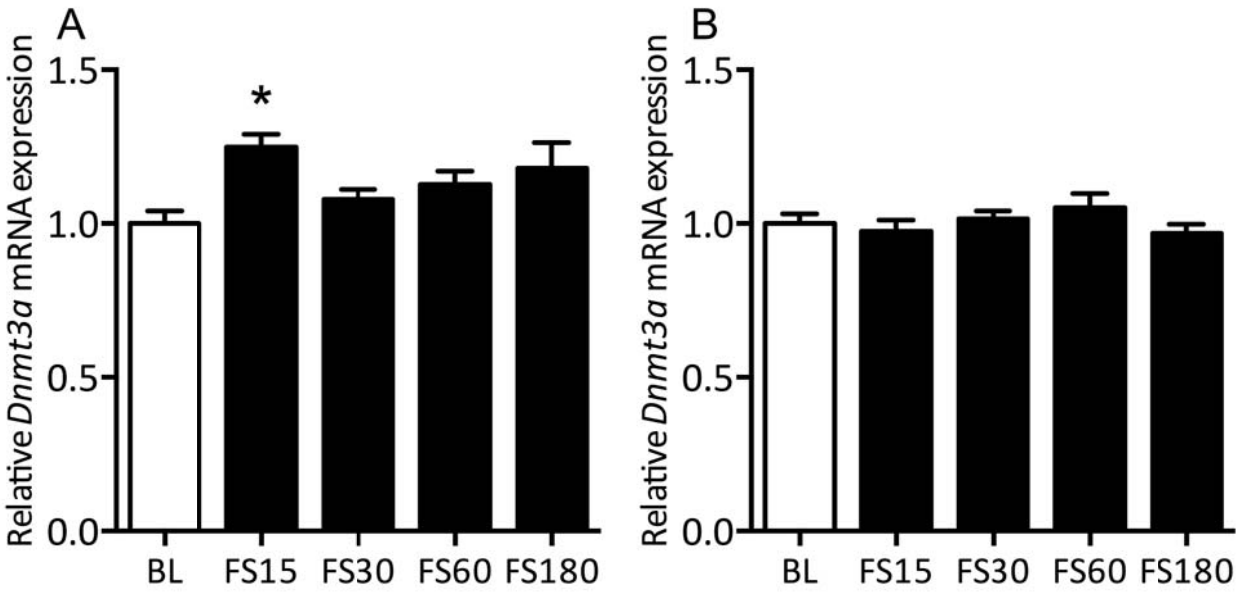
A
B
Relative Dnmt3a mRNA expression
1.5
1.0
0.5
0.0
*
BL
FS15
FS30
FS60
FS180

Figure 8

Figure 9

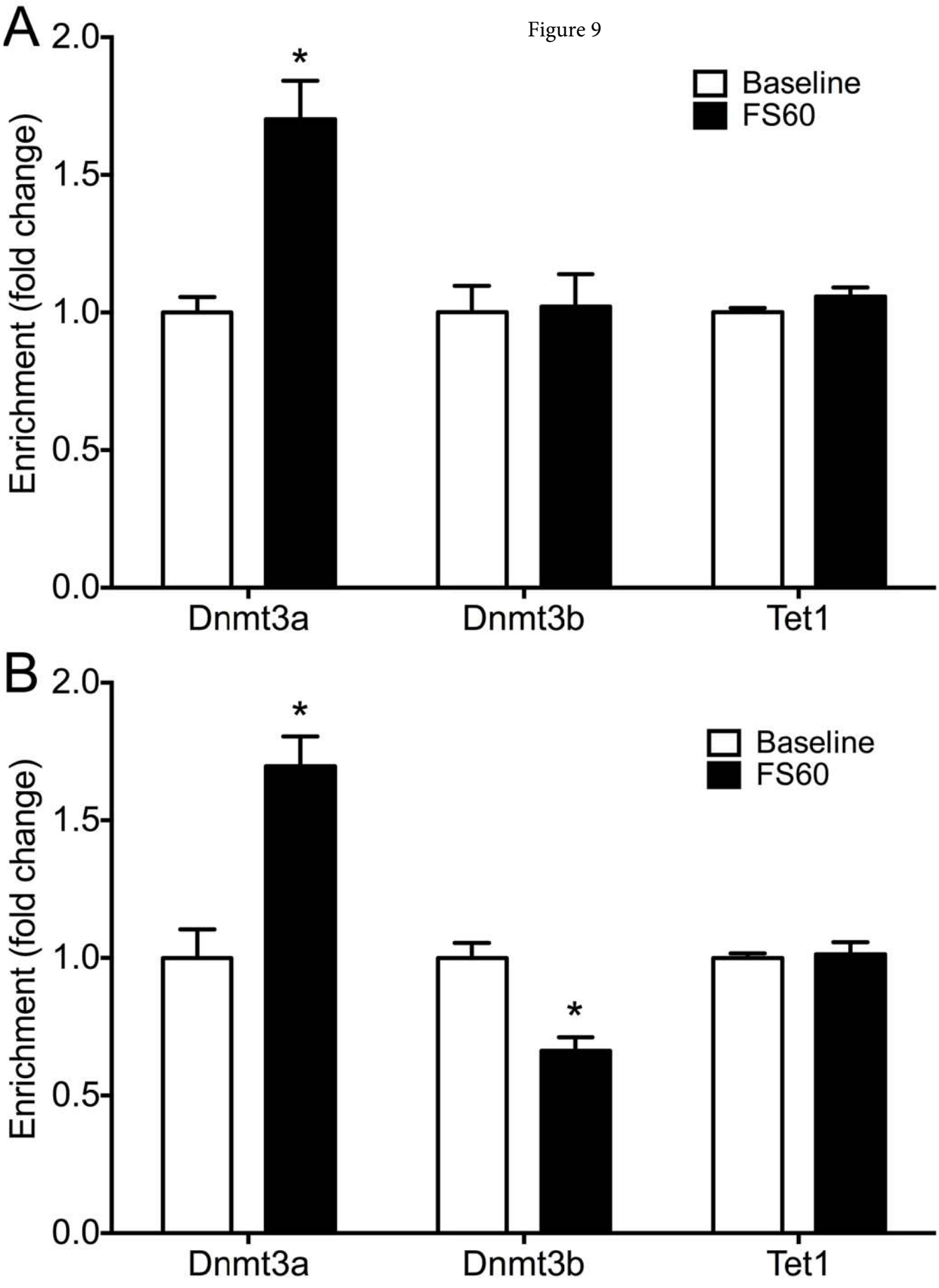
A
2.0
1.5
1.0
0.5
0.0
Enrichment (fold change)
*
Baseline
FS60
Dnmt3a
Dnmt3b
Tet1
B
2.0
1.5
1.0
0.5
0.0
Enrichment (fold change)
*
*
Baseline
FS60
Dnmt3a
Dnmt3b
Tet1

SI Manuscript file

1. SI Materials and Methods

Animals

Male Wistar rats (150-175 g; purchased from Harlan (Oxon, UK)) were group housed (two to three animals per cage) under standard lighting (80-100 Lux; 14:10 light-dark cycle; lights on 05:00) and environmentally controlled conditions (temperature 22 ± 1 °C; relative humidity 50 ± 10%) with food and water available ad libitum. All rats were handled for at least 5 days (3 min/rat/day) before the day of the experiment to reduce non-specific stress. All procedures were approved by the University of Bristol Ethical Committee and by the Home Office of the United Kingdom (UK Animal Scientific Procedures Act 1986).

Drug Treatment

S-adenosyl methionine (SAM; Abbott Laboratories, Maidenhead, UK; 100 mg/kg) was dissolved in sterile pyrogen-free phosphate-buffered saline (PBS) and injected subcutaneously (s.c.). The dose of the drug was based on a previous study（18）. Control animals received a vehicle injection (1 ml/kg, sterile pyrogen-free PBS). The injection was given 30 min before the start of the initial forced swim session. Unless otherwise stated, drugs and chemicals were purchased from Sigma-Aldrich (Poole, UK).

Animal Experimentation

Animal experimentation was conducted between 08:00-13:00. Rats were forced to swim for 15 min in individual glass beakers (height 35 cm, diameter 21.7 cm) containing water 21 ± 2 cm deep at 25 °C or were left undisturbed in their home cage. For experiments involving SAM treatment, animals were given a single s.c. injection of SAM or vehicle 30 min before forced swimming and were killed either at 1 hour after the start of forced swimming or were subjected to a second forced swim (re)test 24 hours later with the same test conditions. Vehicle or SAM injected baseline animals were

killed at the corresponding time after injection. For experiments without drug treatment, animals were killed at indicated times (see figure legends) after forced swimming.

Behavioral Scoring

Behavior in the forced swim test and retest was digitally recorded and scored in a blind fashion, as previously described（5，11）. Behavior (immobility, climbing or swimming) was scored every 10 seconds during the first 5 min of the test and retest, resulting in 30 data bins.

Immunohistochemistry

Brain tissue for immunohistochemistry was collected from rats that were deeply anesthetized with pentobarbital (1 ml/kg) and trans-cardially perfused with ice-cold saline (0.9% w/v sodium chloride (NaCl)) followed by ice-cold buffered formaldehyde solution (4% w/v, 0.195% w/v picric acid, 50 mM sodium fluoride (NaF), 1 mM sodium orthovanadate (Na_3VO_4), 0.1 M phosphate buffer (PB, pH 7.4)). Whole brains were removed and transferred to PB (0.1 M, 50 mM NaF, 1 mM Na_3VO_4, 0.05% w/v sodium azide (NaN_3), pH 7.4) before being cut into 50 µm-thick coronal sections using a vibratome (VT 1000S; Leica, Milton Keynes, UK), and stored at 4 °C until use.

Three brain sections containing the dorsal hippocampus were randomly chosen per animal (between -2.92 mm and -3.96 mm from Bregma; Paxinos and Watson rat brain atlas（40）. As described previously (SI4), the avidin-biotin-immuno-peroxidase (ABC) method was used to detect H3S10p-K14ac, c-Fos and Egr-1 immunopositive neurons. All solutions contained 0.1 M PB pH 7.4; brain sections were carefully rinsed between each step with 0.1 M PB and all steps were performed at room temperature.

After incubation in blocking solution (2% w/v bovine serum albumin (BSA), 50 mM glycine, 0.2% v/v TX-100, 0.5% w/v NaN_3, 50 mM NaF, 1 mM Na_3VO_4, 0.1 M PB), sections were incubated overnight

with one of the following: polyclonal rabbit anti- (pRbα) H3S10p (previous work has shown that in hippocampal neurons the H3S10p mark is actually part of the combinatorial H3S10p-K14ac mark（10，19）; 1:300 v/v), pRbα c-Fos (1:10,000 v/v) both from Merck Millipore (Nottingham, UK), pRbα Egr-1 (1:1000 v/v; Cell Signalling Technology, MA, USA). The antibody was diluted in incubating solution (0.8% w/v BSA, 0.1% v/v Triton X-100, 0.5% w/v NaN_3, 50 mM NaF, 1 mM Na_3VO_4, 0.1 M PB). All antibodies have been used by us and others in multiple studies（5，11，19，41，42）.

Next, sections were incubated with biotinylated goat αRb IgG (1:350; Vector Laboratories, Peterborough, UK) and in avidin-biotinylated horseradish peroxidase complex (1:350; Vector Laboratories, Peterborough, UK). After incubation with 3,3'-diaminobenzidine tetrahydrochloride (DAB 0.8 nM, 7.5 mM ammonium chloride, 0.01% v/v nickel chloride, 0.1 M PB) the peroxidase reaction was initiated upon addition of hydrogen peroxide to a final concentration of 0.003% w/v. Sections were mounted on poly-L-lysine coated slides, dehydrated and cover slipped.

H3S10p-K14ac, c-Fos and Egr-1 immunopositive granule neurons in the dentate gyrus and Egr-1 and c-Fos immunopositive pyramidal neurons in the CA1 and CA3 were counted in a blind fashion using a light microscope (Leica, Milton Keynes, UK). For each animal the positively stained neurons in three brain sections were counted and averaged. The immunopositive granule neurons in the dentate gyrus were counted discriminating between the dorsal and ventral blade. Data are expressed as the mean (± SEM) number of immunopositive neurons per dentate gyrus, CA1 or CA3 in a 50 µm-thick brain section per animal.

Bisulfite Pyrosequencing

For bisulfite pyrosequencing studies and RNA analysis (see below), rats were rapidly anesthetized using isoflurane vapor (< 15 s; Meriam Animal Health Ltd., UK) and decapitated. Next, the brain was removed and immediately cut into 1 mm coronal slices using an ice-cold brain matrix and the slices were placed onto ice-cold steel boxes. Using a preparative light microscope (Leica, Milton Keynes,

UK) the dentate gyrus and the hippocampal CA regions (CA_{1-3}) were micro-dissected from the dorsal hippocampus region and collected in separate tubes on dry ice and stored at -80 °C.

Dentate gyrus and hippocampal CA regions tissue was lysed in 10 volumes of lysis buffer (0.5% w/v SDS, 0.1 M EDTA, 10 mM Tris HCl pH 8.0), before incubation with RNase A (0.05 µg/µl) and proteinase K (0.25 µg/µl). Genomic DNA was purified using a standard phenol-chloroform method and precipitated. Genomic DNA from dentate gyrus and hippocampal CA regions were subjected to bisulfite conversion in duplicate using the EZ DNA methylation kit (Zymo Research, CA, USA) following the manufacturer's instructions. Fully methylated and unmethylated rat DNA controls (EpigenDx, MA, USA) were included along with negative water controls in all experimental steps.

The UCSC Genome Browser and BLAT alignment tool（43，44）were used to identify locations of interest within the c-*Fos* and *Egr-1* genes. Two areas surrounding each gene were selected for primer design, a region within the CpG island located upstream of the transcriptional start site (TSS), and within the region coding for the 5' untranslated region of the mRNA. PCR and sequencing primers were designed using PyroMarkAssayDesign2.0 (Qiagen). Sequences were as follows: c-*Fos* Area 1, forward primer Bt-GTAGAGTTGATGATAGGGAGTT, reverse primer ACTCTATCCAATCTTCTCAATTAC, sequencing primer CTATCCAATCTTCTCAATTACTAA. c-*Fos* Area 2, forward primer GTAGTTAGTAATTGAGAAGATTGGATAGA, reverse primer Bt-CCAAAAATAAACACTAATAAAAACTAC, sequencing primer TGAGAAGATTGGATAGAG. *Egr-1* Area A, forward primer GGGTTTGGGTTTTTTTAGTTTAG, reverse primer Bt-CCCTCCCCCTCCTTAATT, sequencing primer TTTGGGTTTTTTTAGTTTAGT. *Egr-1* Area B, forward primer GTTAGTTTGGGGGTTTATTTATATTTT, reverse primer Bt-TCAACAACATCATCTCCTCCAATTTA, sequencing primer GTTTATTATTTAATATTAGT.

Bisulfite-treated DNA was added to a mastermix (1x reaction buffer, 25 mM $MgCl_2$, 0.5 units HotStar Taq (Qiagen, Manchester, UK) 200 nM of each deoxynucleoside triphosphate (dNTP; Fisher Scientific, Loughborough, UK), 0.25 µM forward and reverse primers) and amplified in duplicate using a thermo cycler (T-100, Biorad, UK). Following purification, DNA methylation was quantified by pyrosequencing using the PyromarkQ24 Pyrosequencer (Qiagen, USA) according to the standard manufacturer's protocol. The data show the mean (± SEM) percentage of DNA methylation for each CpG site per experimental group.

Chromatin preparation and ChIP

For chromatin immuno-precipitation (ChIP), rats were rapidly anaesthetised using isoflurane vapor (< 15 s; Meriam Animal Health Ltd., UK) before decapitation and removal of brains for dissection and processing. To prepare tissue for ChIP, the whole hippocampus was dissected on ice-cold steel boxes. Tissue was quickly chopped into ~1 mm^3 pieces before cross-linking. All solutions used during cross-linking procedure contained the following inhibitors: 50 mM NaF, 1 mM Na_2VO_4, 5 ng/ml aprotinin, 0.1 mM PMSF (phenylmethanesulfonylfluoride), 5 mM NaBut (sodium butyrate; Merck Millipore, Nottingham, UK). Tissue was cross-linked in formaldehyde (1% w/v, PBS pH 7.4) for 10 min at room temperature before quenching with glycine at a final concentration of 125 mM. After two washes with ice-cold PBS the tissue was transferred into storage buffer (10 mM Hepes, 10 mM KCl, 1.5 mM $MgCl_2$ (magnesium chloride), 0.1 mM EGTA (ethylene glycol tetra-acetic acid), 0.5 mM DTT (dithiothreitol) pH 7.9), snap-frozen in dry ice and stored at -80 °C.

For the preparation of chromatin, if solutions are stated to contain inhibitors, these were as follows: 50 mM NaF, 1 mM Na_2VO_4, 5 ng/ml aprotinin, 0.1 mM PMSF, 5 mM NaBut (Merck Millipore, Nottingham, UK), EDTA-free protease inhibitor cocktail tablet (1 per 10 ml, Roche, Burgess Hill, UK)

and phosphatase inhibitor cocktail tablet (1 per 10 ml, Roche, Burgess Hill, UK). Buffers were kept ice-cold with the exception of the sonication buffer.

Cross-linked hippocampal tissue was homogenised in ice-cold homogenisation buffer (10 mM Hepes, 10 mM KCl, 1.5 mM $MgCl_2$, 0.1 mM EGTA, 0.5 mM DTT, with inhibitors, pH 7.9). After centrifuging (6,000 *g*, 4 °C, 5 min) the supernatant was discarded and the pellet resuspended in lysis buffer (0.25 M sucrose, 0.5% v/v Igepal, 100 mM NaCl, 6 mM $MgCl_2$, 0.5 mM DTT, 1 mM EGTA, 50 mM Tris, inhibitors, pH 8.0) and incubated on ice. The samples were mechanically lysed using a 25 gauge needle (Becton, Dickinson and Company, New Jersey, USA). After centrifugation (2,000 *g*, 4 °C, 5 min) the top two layers were discarded leaving the pellet, which was resuspended in homogenisation buffer and layered onto a sucrose cushion (1.2 M sucrose, 100 mM NaCl, 6 mM $MgCl_2$, 1 mM EGTA, 50 mM Tris, 0.5 mM DTT, inhibitors, pH 8.0) before centrifugation (10,000 *g*, 4 °C, 30 min). The remaining sample on top of the sucrose cushion was placed on a second cushion and the centrifugation step repeated. The pellet was resuspended in sonication buffer (1% w/v SDS, 10 mM EDTA, 50 mM Tris, inhibitors, pH 8.0) and sonicated using a water-cooled (4°C) Bioruptor (UCD-300; Diagenode, Liège, Belgium) for 10 cycles (high power, 30 seconds on, 60 seconds off). Samples were removed from the Bioruptor, briefly vortexed and sonicated for a further 10 cycles. Small aliquots of all samples were run on an agarose gel to confirm chromatin was sheared to 1-4 nucleosomes in size (~150-600 bps).

ChIP was performed using the method of Stock et al.（38）with modifications. 20 µl of chromatin was diluted in 180 µl of water to be used as the input. For IP, 150 µg of chromatin was mixed with dilution buffer (50 mM NaCl, 1 mM EDTA, 10 mM Tris, inhibitors, pH 7.4) to a final volume of 1 ml. One of the following antibodies was added to the chromatin mixture: mRbα H3K4me3, pRbα H3K9me3, pRbα H3K27me3 (1:50 v/v; Merck Millipore, Nottingham, UK; these antibodies were verified for specificity by Egelhofer et al.（45）) or rabbit IgG (1:50 v/v; CST, MA, USA) was added and

the samples rolled overnight at 4 °C. Next, the chromatin/Ab mix was incubated with pre-blocked protein A-coated magnetic beads (30 mg/ml; Life Technologies, Paisley, UK) for 3 hours at 4 °C. Beads were collected using a magnetic rack (New England Biolabs, Hitchin, UK) and washed several times to reduce non-specific binding: 2 x wash buffer 1 (0.1% w/v SDS, 1% v/v Triton X-100, 2 mM EDTA, 150 mM NaCl, 20 mM Tris pH 8.0), 2 x wash buffer 2 (0.1% w/v SDS, 1% v/v Triton X-100, 2 mM EDTA, 500 mM NaCl, 20 mM Tris pH 8.0), 1 x wash buffer 3 (1 mM EDTA, 150 mM LiCl, 0.5% v/v Igepal, 0.5% w/v sodium deoxycholate, 20 mM Tris pH 8.0) and finally 2 x TE buffer (1 mM EDTA, 10 mM Tris pH 8.0). The pellets were incubated with elution buffer 1 (1.5% w/v SDS, 50 mM NaCl, 10 mM Tris pH 7.4) followed by a second incubation with elution buffer 2 (0.5% w/v SDS, 50 mM NaCl, 10 mM Tris pH 7.4) after which the supernatants (i.e. the bound fractions) were pooled. NaCl was added to all samples to a final concentration of 150 mM before heating overnight at 65°C to reverse the cross-links.

The bound and input fractions were sequentially incubated with RNase A and proteinase K. Next, the DNA was purified using the phenol-chloroform method. To precipitate the DNA, glycogen was added to a final concentration of 0.1 µg/µl as a co-precipitant before addition of 1/10th the volume of sodium acetate (3 M, pH 5.2) and 3 volumes of ice-cold ethanol (EtOH; 100%), then samples were stored at -20 °C overnight. Next, the DNA pellets from the bound and input samples were collected and washed (70% EtOH) before being resuspended in nuclease-free water and quantified using a Qubit 2.0 Fluorometer (Life Technologies, Paisley, UK).

The Dnmt3a, Dnmt3b and Tet1 ChIP were conducted using a slightly different protocol, which was published recently（7）. The following ChIP-grade antibodies were used: pRbα Tet1 (1:200 v/v; Merck Millipore), pRbα Dnmt3a (1:200 v/v; Abcam), and mMsα Dnmt3b (1:200 v/v; Abcam).

Bound DNA and input DNA were subjected to quantitative polymerase chain reaction (qPCR) using a StepOnePlus machine (Life Technologies, Paisley, UK) and each sample was run in triplicate. DNA was added to a mastermix (900 nM forward and reverse primers, 200 nM probe, 1X TaqMan fast

mastermix (Life Technologies, Paisley, UK), nuclease-free water)). Primers and probe sequences were as follows: c-*Fos*, forward primer CGCTCATGACGTAGTAAGCCATT, probe 6FAM-CGGCCAGCTGAGGCGCCTACT-TAMRA, reverse primer CTGCAATCGCGGTTGGA. *Egr-1*, forward primer GACCCGGAAACACCATATAAGG, probe 6FAM-AAGGATCCCCCGCCGGAACAG-TAMRA, reverse primer AAGGCGCTGCCCAAATAAG.

A standard curve was constructed for each amplicon using whole rat brain genomic DNA (100 ng/µl; BioChain, CA, USA), and run in parallel. The amount of target DNA in the bound and input fractions was calculated by comparing the Ct (cycle threshold) values of these samples to the standard curve. The data are expressed as the ratio of [bound fraction / (input fraction / 20)] and the mean (± SEM) was calculated.

RNA analysis

RNA extraction from dentate gyrus and rest of hippocampus tissue was performed using the guanidinium thiocyanate-phenol-chloroform (TRI) extraction method（39）. Tissue was homogenized in TRI reagent and and centrifuged (12,000 g, 10 min, 4 °C) to remove insoluble material. The supernatant was removed and samples were allowed to stand at room temperature for 15 min. Then, 1-bromo-3-chloropropane was added and the sample shaken vigorously. Next, the samples were centrifuged (12,000 *g*, 15 min, 4 °C) and the upper phase (RNA) removed. After adding 2-propanol and centrifuging (12,000 *g*, RTP) the pellet was washed and resuspended in nuclease-free water (Life Technologies, Paisley, UK) before quantification using a NanoPhotometer P300 (Implen, München, Germany). The RNA integrity was checked using a Bioanalyser (Agilent Technologies, CA, USA). RNA was converted to cDNA using a thermo cycler (T-100, Biorad, UK) and a reverse transcription kit (QuantiTect Reverse Transcription Kit, Qiagen, Manchester, UK) according to the manufacturer's protocol.

For qPCR, 2 µl of cDNA was used per reaction in 18 µl of mastermix (900 nM forward and reverse primers, 200 nM probe, 1X TaqMan fast mastermix (Life Technologies, Paisley, UK), nuclease-free water) using a StepOnePlus machine (Life Technologies, Paisley, UK). Primers and probe as follows: *Dnmt1*, forward primer CAAAGCAAGTGCAATCCCAAA, probe 6FAM-CAACCCGCCACAGTGCCCTGAG-TAMRA, reverse primer TCAGGTCAGGGTCATCTAGGTACTG. *Dnmt3a*, forward primer AAGGTCAAGGAGATCATTGATGAAC, probe 6FAM-TGCGCCAGAAGTGCCGAAACATC-TAMRA, reverse primer CATTGAGGCTCCCACATGAGAT. *Dnmt3b*, forward primer CCTGGCATGTAACCCAGTGA, probe 6FAM-TCGACGCCATCAAGGTTTCTGCTG-TAMRA, reverse primer GGCCTGTTCATTCCAGGTAGAT. For Tet1 mRNA, the AB Taqman gene expression assay Rn01428192 was used.

At least 3 standard curves were run for each primer pair and the average qPCR efficiency was calculated using the equation: $E = (10^{-1/slope}) - 1) \times 100$ (where E is qPCR efficiency and the slope is the gradient of the standard curve). The relative mRNA expression ratio was calculated using the Pfaffl method of relative quantification（46）and standardized to the housekeeping genes *Hprt1* and *Ywhaz*. The data was normalized to the baseline group and shown as the mean (± SEM) relative mRNA expression.

Statistical Analysis

The data was statistically analyzed using analysis of variance (ANOVA) and, and in case of a significant main effect, differences between individual groups were evaluated with appropriate post-hoc tests, adjusting the level of significance according to the Bonferroni procedure to reduce the probability of a type 1 error. Some data were analyzed using Student's t-test. Results shown are mean ± SEM, with $p<0.05$ considered statistically significant.

2. SI Figure Legends

Figure S1. Representative images of c-Fos immuno-staining in the dentate gyrus of SAM-treated, forced swim-challenged rats. Rats were s.c. injected with vehicle or SAM (100mg/kg) and either killed under baseline conditions ('Control') or 60 min after start of a 15-min forced swim (FS) challenge. (a-d) show representative images of the four treatment conditions with low-magnification images shown at the left side and, on the right side, higher magnification images of the indicated rectangles depicted in the respective left-sided images. The black arrows indicate examples of positively stained dentate gyrus neuronal nuclei. GCL, granular cell layer

Figure S2. The effect of SAM on forced swimming-evoked c-Fos and Egr-1 induction in the dentate gyrus. Rats were given one injection of vehicle or SAM (100 mg/kg, s.c.) 30 min before forced swimming (15 min, 25°C) and killed 60 min after the start of the challenge (FS60). The baseline (BL) groups were killed 90 min after injection. The graphs show the number of c-Fos$^+$ and Egr-1$^+$ neurons split between the dorsal and the ventral blade (A and B, respectively). Representative images of c-Fos$^+$ (C) and Egr-1$^+$ (D) neurons in the dorsal blade of the dentate gyrus under baseline (BL) or stress conditions (FS60)) are shown. ML; molecular layer, GCL; granular cell layer, H; hilus. Data in A-B are shown as the average number of c-Fos$^+$ or Egr-1$^+$ neurons from three, 50 µm-thick coronal brain slices per animal (mean ± SEM, n = 5-6). (A) Three-way ANOVA; effect of SAM: $F_{(1,36)} = 19$, $p < 0.0001$; effect of stress: $F_{(1,36)} = 130$, $p < 0.0001$; effect of location: $F_{(1,36)} = 600$, $p < 0.0001$; interaction SAM x stress: $F_{(1,36)} = 34$, $p < 0.0001$; interaction of SAM x location: $F_{(1,36)} = 15$, $p < 0.0001$; interaction stress x location: $F_{(1,36)} = 80$, $p < 0.0001$; interaction SAM x stress x location: $F_{(1,36)} = 14$, $p < 0.01$. (B) Three-way ANOVA; effect of SAM: $F_{(1,36)} = 9.4$, $p < 0.01$; effect of stress: $F_{(1,36)} = 6.3$, $p < 0.05$; effect of location: $F_{(1,36)} = 170$, $p < 0.0001$; interaction SAM x stress: $F_{(1,36)} = 8.1$, $p < 0.01$; interaction of SAM x location: $F_{(1,36)} = 5.5$, $p < 0.05$; interaction stress x location: $F_{(1,36)} = 8.6$, $p < 0.01$; interaction SAM x stress x location: $F_{(1,36)} = 8.4$, $p < 0.01$. Bonferroni-corrected post-hoc test with contrasts: *, $p < 0.05$

compared with the respective BL group; $, p < 0.05 compared with the respective vehicle/FS60 group; #, p < 0.05 compared with the respective ventral blade group

Figure S3. The effect of SAM on forced swimming-induced c-Fos and Egr-1 induction in the CA1 and CA3. Rats were given one injection of vehicle or SAM (100 mg/kg, s.c.) 30 min before forced swimming (15 min, 25°C) and killed 60 min after the start of the challenge (FS60). The baseline (BL) groups were killed 90 min after the injection. The graphs show the number of c-Fos$^+$ and Egr-1$^+$ neurons in the CA1 (A and B, respectively) and the CA3 (C and D, respectively). Data are shown as an average number of c-Fos$^+$ or Egr-1$^+$ neurons from two, 50 µm-thick coronal brain slices per animal (mean ± SEM, n = 3-4). Statistical analysis: two-way ANOVA; (A) effect of SAM: $F_{(1,12)} = 0.91$, $p = 0.36$; effect of stress: $F_{(1,12)} = 43$, $p < 0.0001$; interaction SAM x stress: $F_{(1,12)} = 1.1$, $p = 0.31$. (B) Effect of SAM: $F_{(1,12)} = 0.24$, $p = 0.63$; effect of stress: $F_{(1,12)} = 5.1$, $p < 0.05$; interaction SAM x stress: $F_{(1,12)} = 0.12$, $p = 0.73$. (C) Effect of SAM: $F_{(1,11)} = 0.61$, $p = 0.45$; effect of Stress: $F_{(1,11)} = 1.6$, $p = 0.23$; interaction SAM x stress: $F_{(1,11)} = 0.042$, $p = 0.84$. (D) Effect of SAM: $F_{(1,14)} = 0.082$, $p = 0.78$; effect of stress: $F_{(1,14)} = 2.6$, $p = 0.13$; interaction SAM x stress: $F_{(1,14)} = 0.34$, $p = 0.57$. Bonferroni-corrected post-hoc test with contrasts: *, $p < 0.05$ compared with the respective BL group

Figure S4. The effect of SAM on H3S10p-K14ac formation in the dentate gyrus after forced swimming. Rats were given one injection of vehicle or SAM (100 mg/kg, s.c.) 30 min before forced swimming (15 min, 25°C) and killed at FS60. The BL groups were killed 90 min after the injection. The graphs show the number of H3S10p-K14ac$^+$ neurons split between the dorsal and the ventral blade (A). Representative images of H3S10p-K14ac$^+$ (B) neurons in the dorsal blade of the dentate gyrus under baseline (BL) or stress conditions (FS60) are shown. ML; molecular layer, GCL; granular cell layer, H; hilus. Data in A are shown as an average number of H3S10p-K14ac$^+$ neurons from three, 50 µm-thick coronal brain slices per animal (mean ± SEM, n = 4-6). (A) Three-way ANOVA; effect of

SAM: $F_{(1,32)} = 0.33$, $p = 0.57$; effect of stress: $F_{(1,32)} = 28$, $p < 0.0001$; effect of location: $F_{(1,32)} = 50$, $p < 0.0001$; interaction SAM x stress: $F_{(1,32)} = 0.0049$, $p = 0.95$; interaction of SAM x location: $F_{(1,32)} = 0.22$, $p = 0.65$; interaction stress x location: $F_{(1,32)} = 11$, $p < 0.01$; interaction SAM x stress x location: $F_{(1,32)} = 0.053$, $p = 0.82$. Bonferroni-corrected post-hoc test with contrasts: *, $p < 0.05$ compared with the respective BL group; #, $p < 0.05$ compared with the respective ventral blade group

Figure S5. Forced swimming-induced CpG-specific DNA methylation changes in the c-*Fos* promoter region in the CA regions of the hippocampus. Rats were killed immediately (BL group) or subjected to forced swimming (15 min, 25°C) and killed at FS60. The location of CpGs within Areas 1 and 2 with respect to the rat c-*Fos* gene are shown in (A). The graph shows DNA methylation changes at CpGs in Area 1 and Area 2 in the CA regions of the dorsal hippocampus (B). Data are shown as percentage methylation (mean ± SEM, n = 3-6). (B) Area 1; effect of CpG number: $F_{(6,54)} = 28$, $p < 0.0001$; effect of stress: $F_{(1,54)} = 0.030$, $p = 0.87$; interaction CpG number x stress: $F_{(6,54)} = 0.44$, $p = 0.85$. Area 2; effect of CpG number: $F_{(6,60)} = 43$, $p < 0.0001$; effect of stress: $F_{(1,60)} = 0.73$, $p = 0.41$; interaction CpG number x stress: $F_{(6,60)} = 1.2$, $p = 0.30$. Student's t-test: *, $p < 0.05$; &, $p < 0.1$, compared with the respective BL group

Figure S6. Forced swimming-induced CpG-specific DNA methylation changes in the *Egr-1* promoter region in the CA regions of the hippocampus. Rats were killed immediately (BL group) or subjected to forced swimming (15 min, 25°C) and killed at FS60. The location of CpGs within Areas A and B with respect to the rat *Egr-1* gene is shown in (A). The graphs show DNA methylation changes at CpGs in Area A and Area B in the CA regions of the dorsal hippocampus (B). Data are shown as percentage methylation (mean ± SEM, n = 5-6). *, $p < 0.05$; &, $p < 0.1$, compared with the respective BL group. Statistical analysis: two-way ANOVA with repeated measures; (B) Area A; effect of CpG number: $F_{(16,160)} = 71$, $p < 0.0001$; effect of stress: $F_{(1,160)} = 0.32$, $p = 0.58$; interaction CpG number x stress: $F_{(16,160)} = 0.63$, $p = 0.85$. Area B; effect of CpG number: $F_{(7,56)} = 360$, $p < 0.0001$; effect of stress: $F_{(1,56)} =$

2.0, p = 0.20; interaction CpG number x stress: $F_{(7,56)}$ = 1.6, p = 0.16. Student's t-test: *, p < 0.05; &, p < 0.1, compared with the respective BL group

Figure S7. The effect of SAM treatment and forced swimming on CpG methylation in the c-*Fos UTR* and *Egr-1* gene promoter in the CA regions of the hippocampus. Rats were given one injection of vehicle or SAM (100 mg/kg, s.c.) 30 min before forced swimming (15 min, 25°C) and killed at FS60. The BL groups were killed 90 min after the injection. The graphs show methylation of CpGs in Area 2 of the *c-Fos* gene promoter (A) and Area A of the *Egr-1* gene promoter (B) from the CA regions. Data are shown as percentage methylation (mean ± SEM, n = 4-6). Statistical analysis: Three-way ANOVA; (A) effect of SAM: $F_{(1,134)}$ = 3.6, p = 0.060; effect of stress: $F_{(1,134)}$ = 18, p < 0.0001; effect of CpG number: $F_{(6,134)}$ = 150, p < 0.0001; interaction SAM x stress: $F_{(1,134)}$ = 28, p < 0.0001; interaction SAM x CpG number: $F_{(5,134)}$ = 0.89, p = 0.49; interaction stress x CpG number: $F_{(6,134)}$ = 1.2, p = 0.31; interaction SAM x stress x CpG number: $F_{(5,134)}$ = 0.42, p = 0.84. (B) Effect of SAM: $F_{(1,280)}$ = 1.9, p = 0.17; effect of stress: $F_{(1,280)}$ = 6.2, p < 0.05; effect of CpG number: $F_{(16,280)}$ = 110, p < 0.0001; interaction SAM x stress: $F_{(1,280)}$ = 0.0, p = 1.0; interaction SAM x CpG number: $F_{(11,280)}$ = 0.47, p = 0.92; interaction stress x CpG number: $F_{(16,280)}$ = 0.83, p = 0.66; interaction SAM x stress x CpG number: $F_{(11,280)}$ = 0.60, p = 0.83. Bonferroni-corrected post-hoc test with contrasts: *, p < 0.05 compared with the respective vehicle/BL group; $, p < 0.05 compared with the respective SAM/BL group

Figure S8. The enrichment of H3K4me3, H3K9me3 and H3K27me3 at the c-*Fos* and *Egr-1* promoters after SAM treatment and forced swimming. Rats were given one injection of vehicle or SAM (100 mg/kg, s.c.) 30 min before forced swimming (15 min, 25°C) and killed at 60 min after start of the stressor (FS60). The BL groups were killed 90 min after the injection. The graphs show the enrichment of H3K4me3 (A), H3K9me3 (C) and H3K27me3 (E) at the c-*Fos* gene promoter, and H3K4me3 (B), H3K9me3 (D) and H3K27me3 (F) at the *Egr-1* gene promoter. Data are shown as a

ratio of target DNA after immunoprecipitation ('Bound') compared with target DNA in the Input sample (A-B mean ± SEM, n = 3; C-F mean and range, n=2). Statistical analysis: two-way ANOVA; (A) effect of SAM: $F_{(1,8)} = 0.036$, p = 0.85, effect of stress: $F_{(1,8)} = 0.85$, p = 0.38, interaction SAM x stress: $F_{(1,8)} = 0.044$, p = 0.84. (B) Effect of SAM: $F_{(1,8)} = 0.42$, p = 0.54, effect of stress: $F_{(1,8)} = 0.92$, p = 0.36, interaction SAM x stress: $F_{(1,8)} = 0.63$, p = 0.45.

Figure S9. Effect of forced swimming on *Dnmt3b*, *Dnmt1* and *Tet1* mRNA expression in the dentate gyrus and CA regions of the hippocampus. Rats were killed immediately (BL group) or subjected to forced swimming (15 min, 25°C) and killed immediately (FS15), 30 min (FS30), 60 min (FS60) or 180 min (FS180) after the start of the challenge. The graphs show *Dnmt3b, Dnmt1 and Tet1* expression in the dentate gyrus (A, C , E) and the CA regions (B, D, F) of the hippocampus. Data are shown as relative mRNA copy number calculated using the Pfaffl method of analysis, standardised to the expression of the house keeping genes *Hprt1* and *Ywhaz* (mean ± SEM, n = 8-9). Statistical analysis: Statistical analysis: one-way ANOVA; (A) $F_{(4,38)} = 2.0$, p = 0.12. (B) $F_{(4,39)} = 0.71$, p = 0.59. (C) $F_{(4,38)} = 0.82$, p = 0.52. (D) $F_{(4,39)} = 1.4$, p = 0.24. (E) $F_{(4, 38)} = 1.71$, p = 0.17 . (F) $F_{(4, 37)} = 0.75$, p = 0.57.

3. SI Statistics Information to main manuscript Figures 1-7

Figure 1. The effect of SAM on forced swimming-induced behaviour

Statistical analysis: two-way ANOVA; (A) effect of behaviour: $F_{(2,45)} = 22$, $p < 0.0001$; effect of SAM: $F_{(1,45)} = 0.0$, $p = 1.0$; interaction behaviour x SAM: $F_{(2,45)} = 0.14$, $p = 0.86$. (B) Effect of behaviour: $F_{(2,45)} = 13$, $p < 0.0001$; effect of SAM: $F_{(1,45)} = 0.0$, $p = 1.0$; interaction behaviour x SAM: $F_{(2,45)} = 6.8$, $p < 0.01$. Bonferroni-corrected post-hoc test with contrasts: *, $p < 0.05$ compared with the respective vehicle-treated group; &, $p = 0.072$ compared with the respective vehicle-treated group.

Figure 2. The effect of SAM on forced swimming-evoked c-Fos and Egr-1 induction in the dentate gyrus

Statistical analysis: (A) two-way ANOVA; effect of SAM: $F_{(1,18)} = 20$, $p < 0.001$; effect of stress: $F_{(1,18)} = 140$, $p < 0.0001$; interaction SAM x stress: $F_{(1,18)} = 37$, $p < 0.0001$. (B) Two-way ANOVA; effect of SAM: $F_{(1,18)} = 10$, $p < 0.01$; effect of stress: $F_{(1,18)} = 6.1$, $p < 0.05$; interaction SAM x stress: $F_{(1,18)} = 6.9$, $p < 0.05$. Bonferroni-corrected post-hoc test with contrasts: *, $p < 0.05$ compared with the respective BL group; $, $p < 0.05$ compared with the respective vehicle/FS60 group; #, $p < 0.05$ compared with the respective ventral blade group

Figure 3. The effect of SAM on H3S10p-K14ac formation in the dentate gyrus after forced swimming

Statistical analysis: two-way ANOVA; effect of SAM: $F_{(1,16)} = 0.24$, $p = 0.63$; effect of stress: $F_{(1,16)} = 20$, $p < 0.001$; interaction SAM x stress: $F_{(1,16)} = 0.0034$, $p = 0.95$. Bonferroni-corrected post-hoc test with

contrasts: *, $p < 0.05$ compared with the respective BL group; #, $p < 0.05$ compared with the respective ventral blade group

Figure 4. Forced swimming-induced CpG-specific DNA methylation changes in the c-*Fos* promoter region

Statistical analysis: two-way ANOVA with repeated measures; Area 1; effect of CpG number: $F_{(6,36)} = 81$, $p < 0.0001$; effect of stress: $F_{(1,36)} = 0.26$, $p = 0.63$; interaction CpG number x stress: $F_{(6,36)} = 0.65$, $p = 0.69$. Area 2; effect of CpG number: $F_{(6,48)} = 39$, $p < 0.0001$; effect of stress: $F_{(1,48)} = 3.1$, $p = 0.12$; interaction CpG number x stress: $F_{(6,48)} = 2.2$, $p = 0.065$. Student's t-test: *, $p < 0.05$; &, $p < 0.1$, compared with the respective BL group.

Figure 5. Forced swimming-induced CpG-specific DNA methylation changes in the *Egr-1* promoter region

Statistical analysis: two-way ANOVA with repeated measures; (B) Area A; effect of CpG number: $F_{(16,160)} = 48$, $p < 0.0001$; effect of stress: $F_{(1,160)} = 4.1$, $p = 0.070$; interaction CpG number x stress: $F_{(16,160)} = 3.1$, $p < 0.001$. Area B; effect of CpG number: $F_{(7,63)} = 370$, $p < 0.0001$; effect of stress: $F_{(1,63)} = 0.37$, $p = 0.56$; interaction CpG number x stress: $F_{(7,63)} = 1.9$, $p = 0.090$. Student's t-test: *, $p < 0.05$; &, $p < 0.1$, compared with the respective BL group.

Figure 6. The effect of SAM treatment on forced swimming-induced DNA methylation changes at CpGs within the c-*Fos* UTR in the dentate gyrus

Statistical analysis: Three-way ANOVA; effect of SAM: $F_{(1,133)} = 1.9$, $p = 0.17$; effect of stress: $F_{(1,133)} = 4.5$, $p = 0.035$; effect of CpG number: $F_{(6,133)} = 99$, $p < 0.0001$; interaction SAM x stress: $F_{(1,133)} = 8.9$, p

< 0.01; interaction SAM x CpG number: $F_{(5,133)} = 1.3$, $p = 0.28$; interaction stress x CpG number: $F_{(6,133)} = 0.91$, $p = 0.49$; interaction SAM x stress x CpG number: $F_{(5,133)} = 1.2$, $p = 0.30$. Bonferroni-corrected post-hoc test with contrasts: *, $p < 0.05$ compared with the respective vehicle/FS60 group; $, $p < 0.05$ compared with the respective SAM/BL group; +, $p = 0.076$ compared with the respective SAM/BL group; &, $p = 0.076$ compared with the respective vehicle/FS60 group.

Figure 7. The effect of SAM treatment on forced swimming-induced DNA methylation changes at CpGs within the *Egr-1* gene promoter in the dentate gyrus

Statistical analysis: Three-way ANOVA; effect of SAM: $F_{(1,255)} = 51$, $p < 0.0001$; effect of stress: $F_{(1,255)} = 5.4$, $p < 0.05$; effect of CpG number: $F_{(16,255)} = 29$, $p < 0.0001$; interaction SAM x stress: $F_{(1,255)} = 17$, $p < 0.0001$; interaction SAM x CpG number: $F_{(11,255)} = 1.9$, $p < 0.05$; interaction stress x CpG number: $F_{(16,255)} = 2.1$, $p < 0.05$; interaction SAM x stress x CpG number: $F_{(11,255)} = 1.9$, $p = 0.051$. Bonferroni-corrected post-hoc test with contrasts: *, $p < 0.05$ compared with the respective vehicle/FS60 group; $, $p < 0.05$ compared with the respective SAM/BL group.

Supplementary figures: **Figure S1**

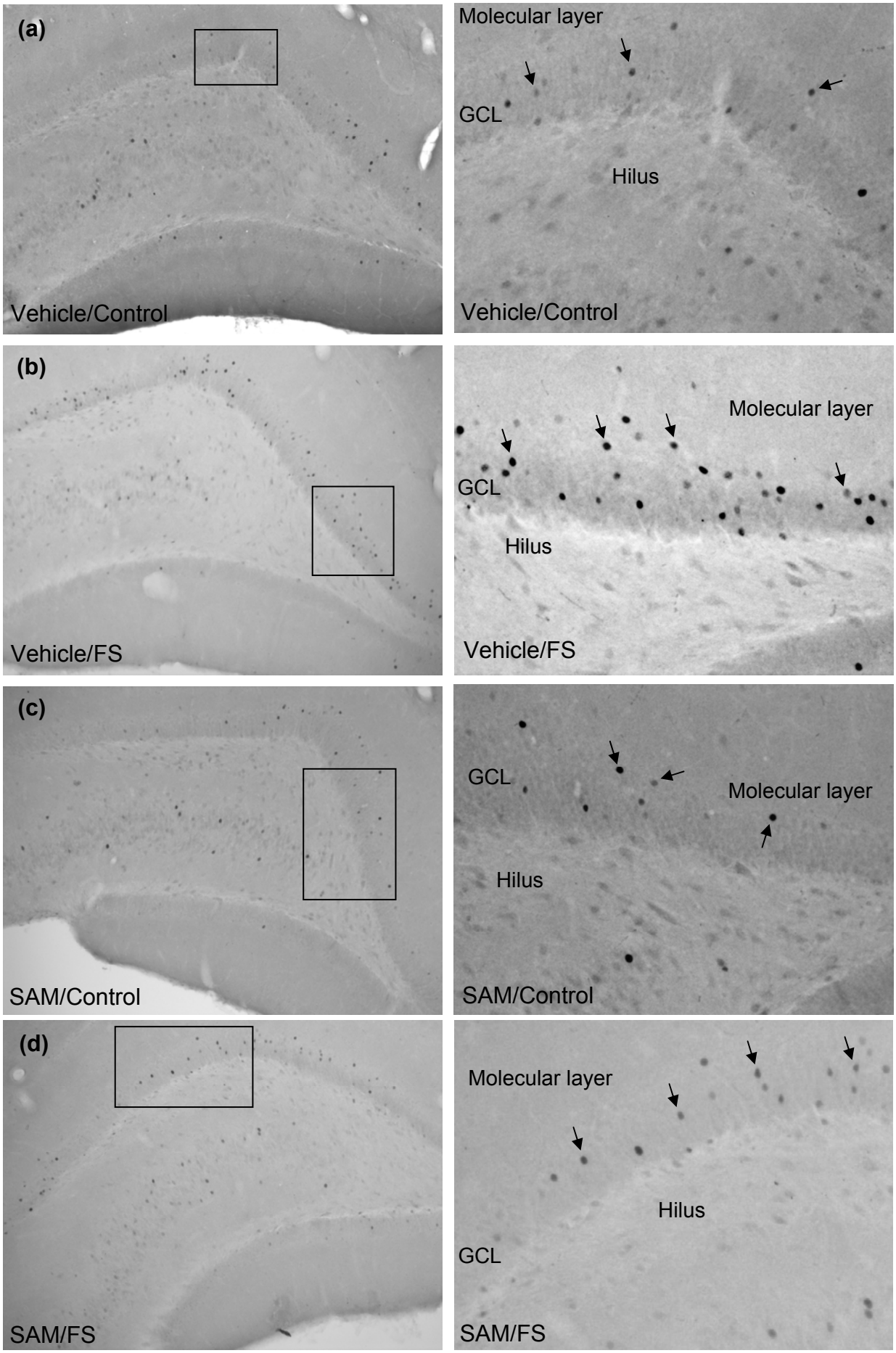

Figure S2

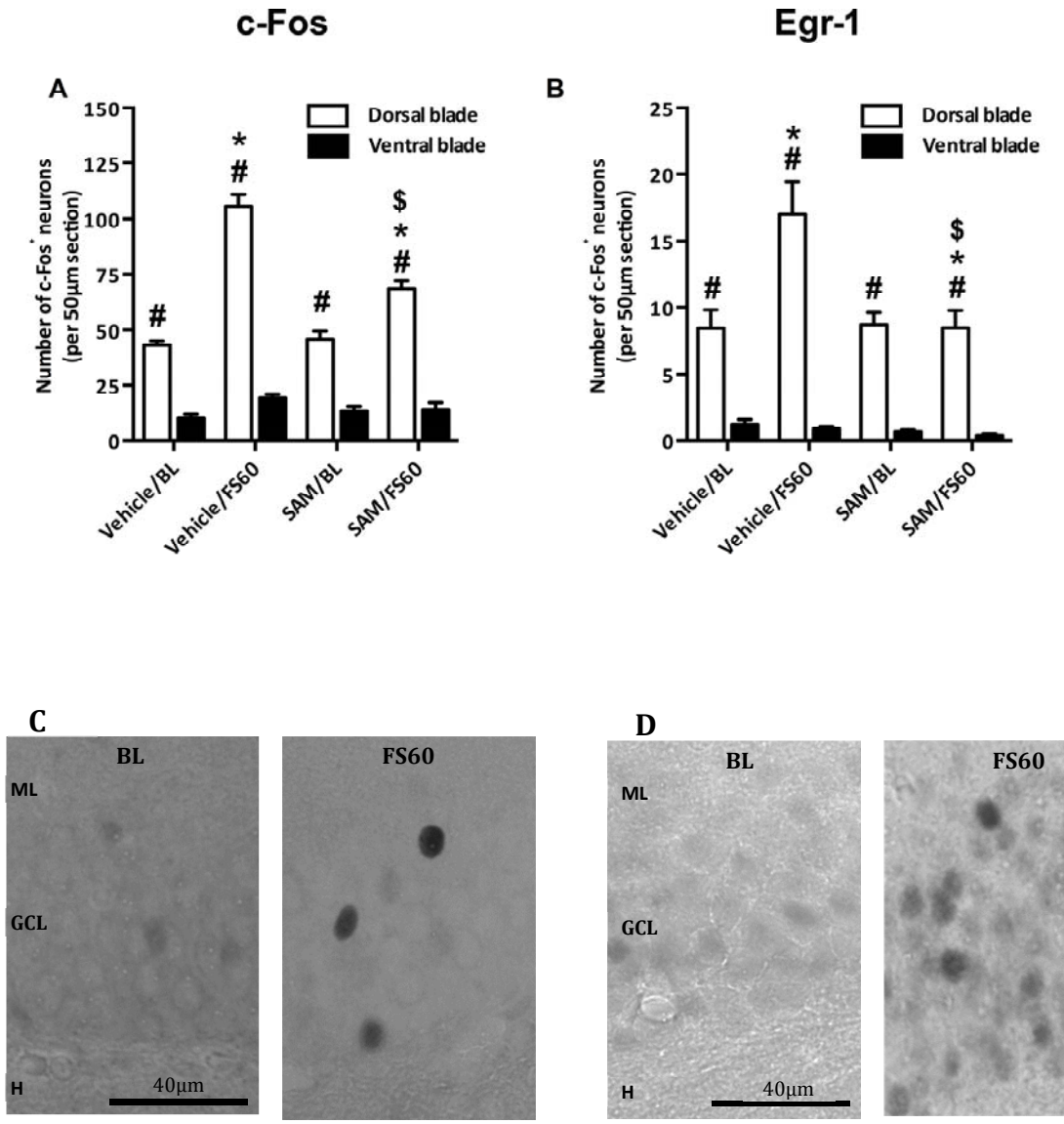
c-Fos
Egr-1
A
B
Dorsal blade
Ventral blade
Number of c-Fos+ neurons (per 50µm section)
Vehicle/BL
Vehicle/FS60
SAM/BL
SAM/FS60
C
D
BL
FS60
ML
GCL
H
40µm

Figure S3.

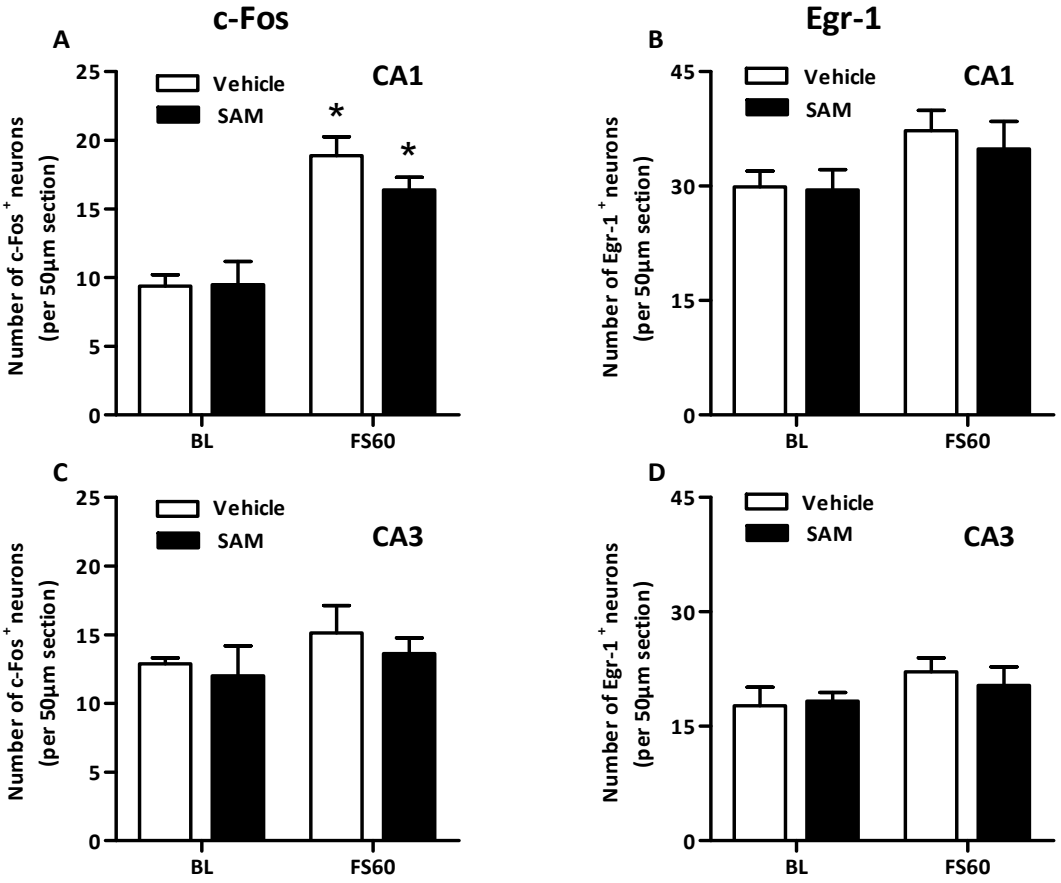
c-Fos
A
CA1
Vehicle
SAM
Number of c-Fos+ neurons (per 50µm section)
25
20
15
10
5
0
*
*
BL
FS60
Egr-1
B
CA1
Vehicle
SAM
Number of Egr-1+ neurons (per 50µm section)
45
30
15
0
BL
FS60
C
CA3
Vehicle
SAM
Number of c-Fos+ neurons (per 50µm section)
25
20
15
10
5
0
BL
FS60
D
CA3
Vehicle
SAM
Number of Egr-1+ neurons (per 50µm section)
45
30
15
0
BL
FS60

Figure S4

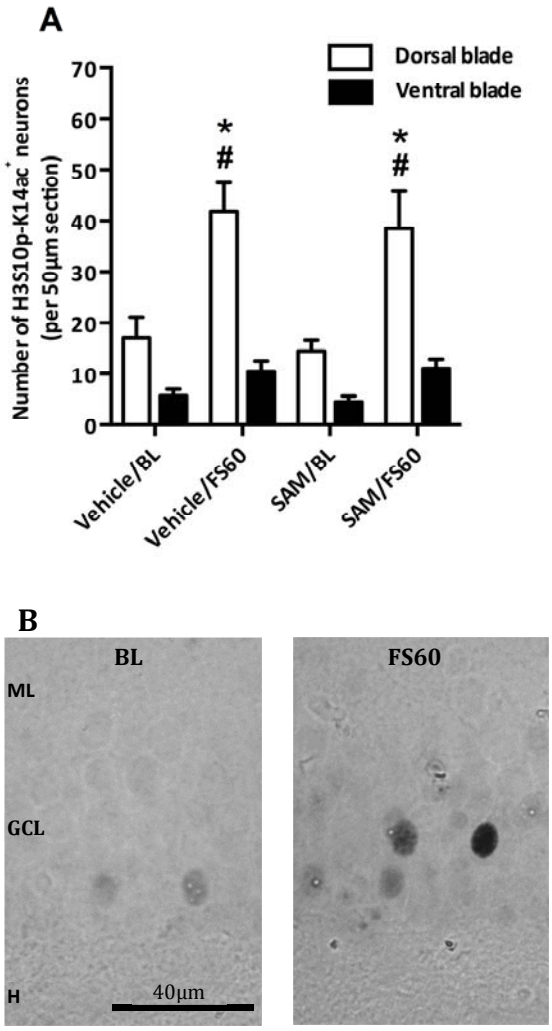
A
Dorsal blade
Ventral blade
Number of H3S10p-K14ac+ neurons (per 50µm section)
70
60
50
40
30
20
10
0
*
#
*
#
Vehicle/BL
Vehicle/FS60
SAM/BL
SAM/FS60
B
BL
FS60
ML
GCL
H
40µm

Figure S5

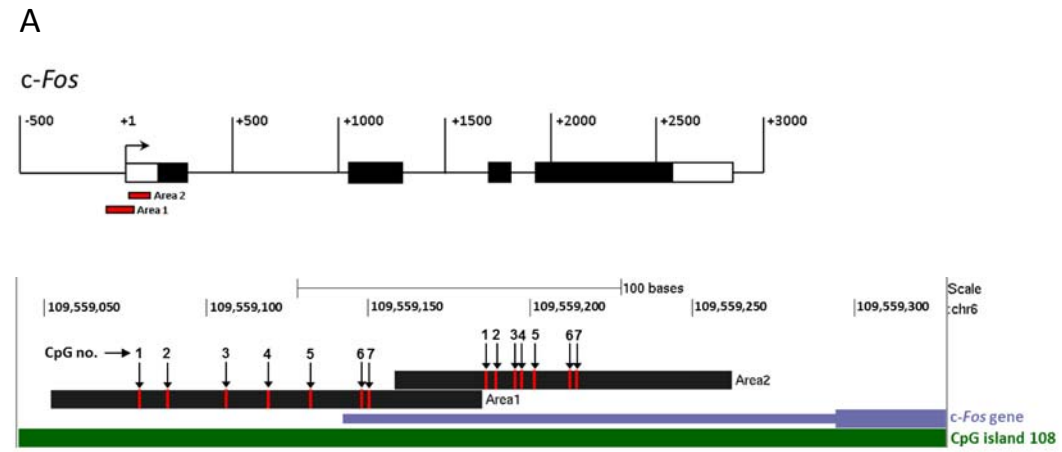
A
c-Fos
-500
+1
+500
+1000
+1500
+2000
+2500
+3000
Area 2
Area 1
100 bases
Scale
chr6
109,559,050
109,559,100
109,559,150
109,559,200
109,559,250
109,559,300
CpG no.
1 2 3 4 5 6 7
1 2 3 4 5 6 7
Area2
Area1
c-Fos gene
CpG island 108

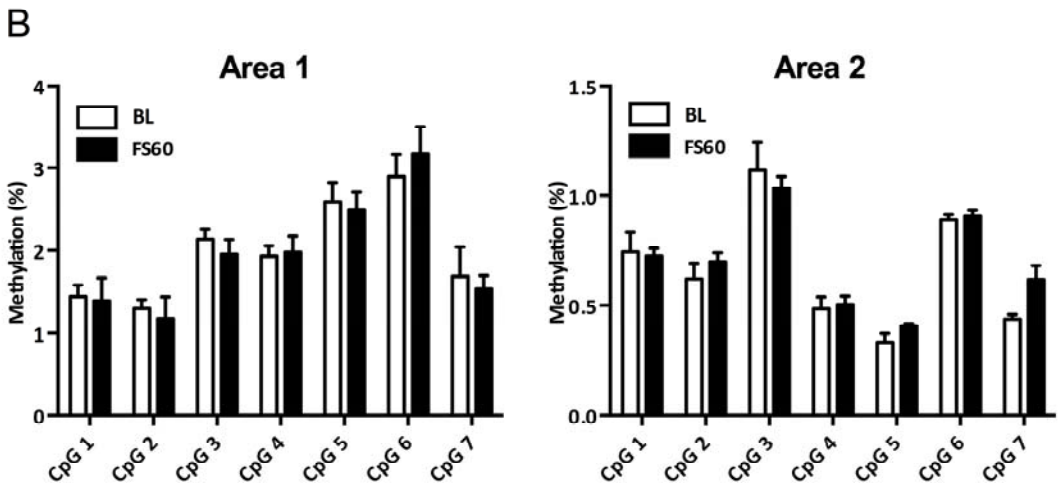
B
Area 1
Area 2
BL
FS60
Methylation (%)
0
1
2
3
4
0.0
0.5
1.0
1.5
CpG 1
CpG 2
CpG 3
CpG 4
CpG 5
CpG 6
CpG 7

Figure S6

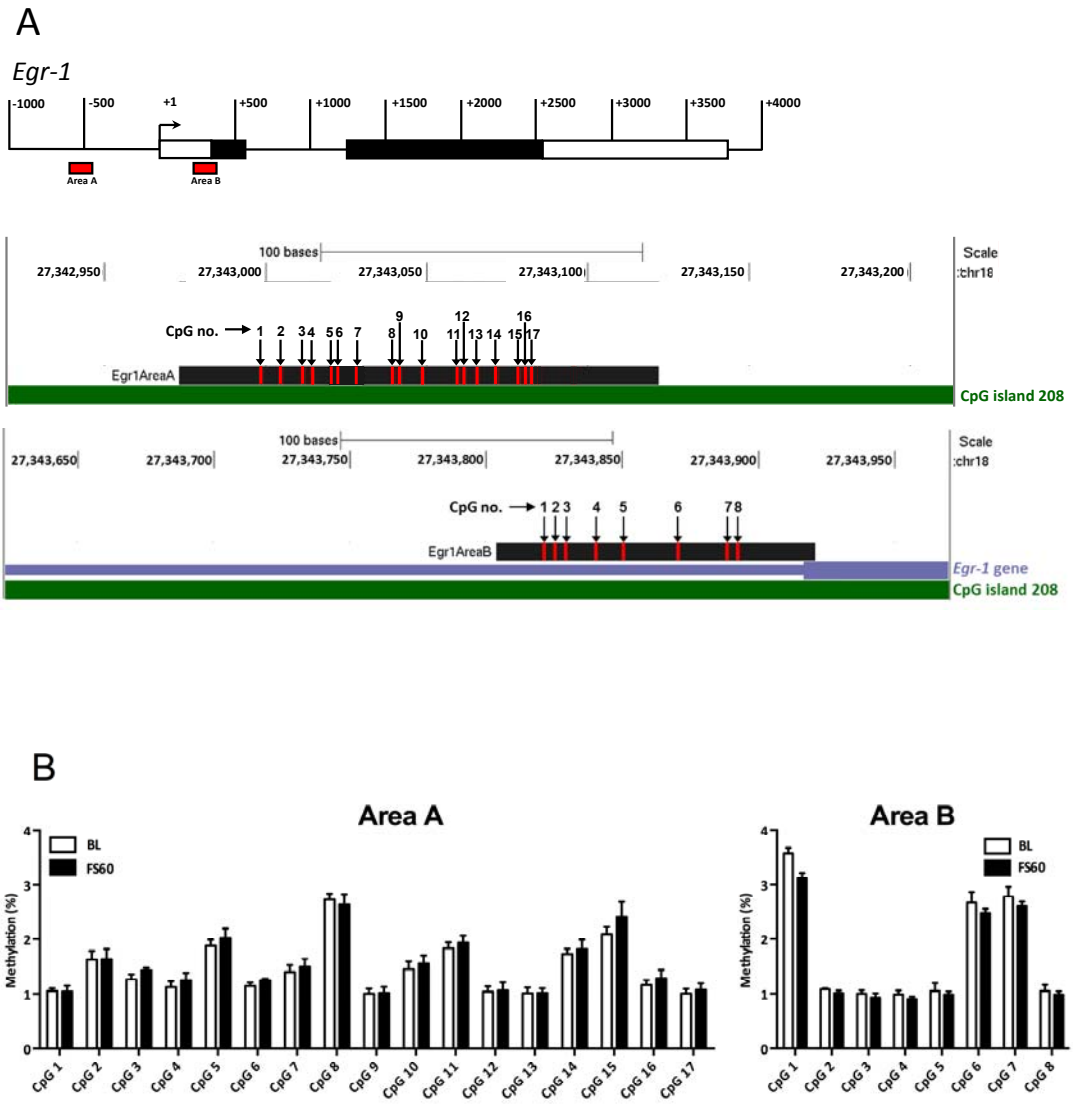
A
Egr-1
-1000
-500
+1
+500
+1000
+1500
+2000
+2500
+3000
+3500
+4000
Area A
Area B
100 bases
27,342,950
27,343,000
27,343,050
27,343,100
27,343,150
27,343,200
Scale
:chr18
CpG no.
1 2 3 4 5 6 7 8 9 10 11 12 13 14 15 16 17
Egr1AreaA
CpG island 208
100 bases
27,343,650
27,343,700
27,343,750
27,343,800
27,343,850
27,343,900
27,343,950
Scale
:chr18
CpG no.
1 2 3 4 5 6 7 8
Egr1AreaB
Egr-1 gene
CpG island 208

B
Area A
Area B
BL
FS60
Methylation (%)
0
1
2
3
4
CpG 1
CpG 2
CpG 3
CpG 4
CpG 5
CpG 6
CpG 7
CpG 8
CpG 9
CpG 10
CpG 11
CpG 12
CpG 13
CpG 14
CpG 15
CpG 16
CpG 17

Figure S7.

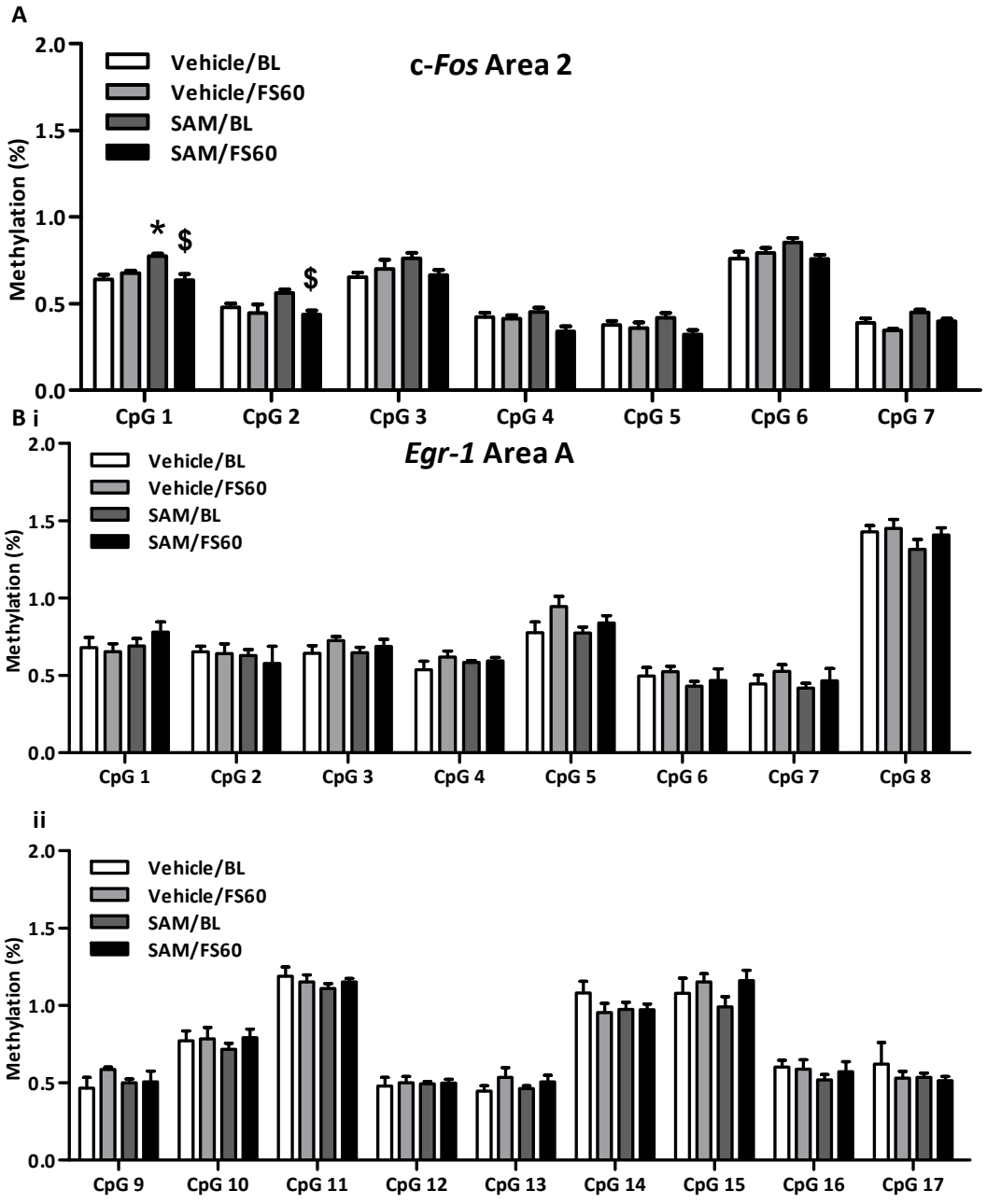
A
c-Fos Area 2
Vehicle/BL
Vehicle/FS60
SAM/BL
SAM/FS60
Methylation (%)
2.0
1.5
1.0
0.5
0.0
*
$
$
CpG 1
CpG 2
CpG 3
CpG 4
CpG 5
CpG 6
CpG 7
B i
Egr-1 Area A
Vehicle/BL
Vehicle/FS60
SAM/BL
SAM/FS60
Methylation (%)
CpG 1
CpG 2
CpG 3
CpG 4
CpG 5
CpG 6
CpG 7
CpG 8
ii
Vehicle/BL
Vehicle/FS60
SAM/BL
SAM/FS60
Methylation (%)
CpG 9
CpG 10
CpG 11
CpG 12
CpG 13
CpG 14
CpG 15
CpG 16
CpG 17

Figure S8.

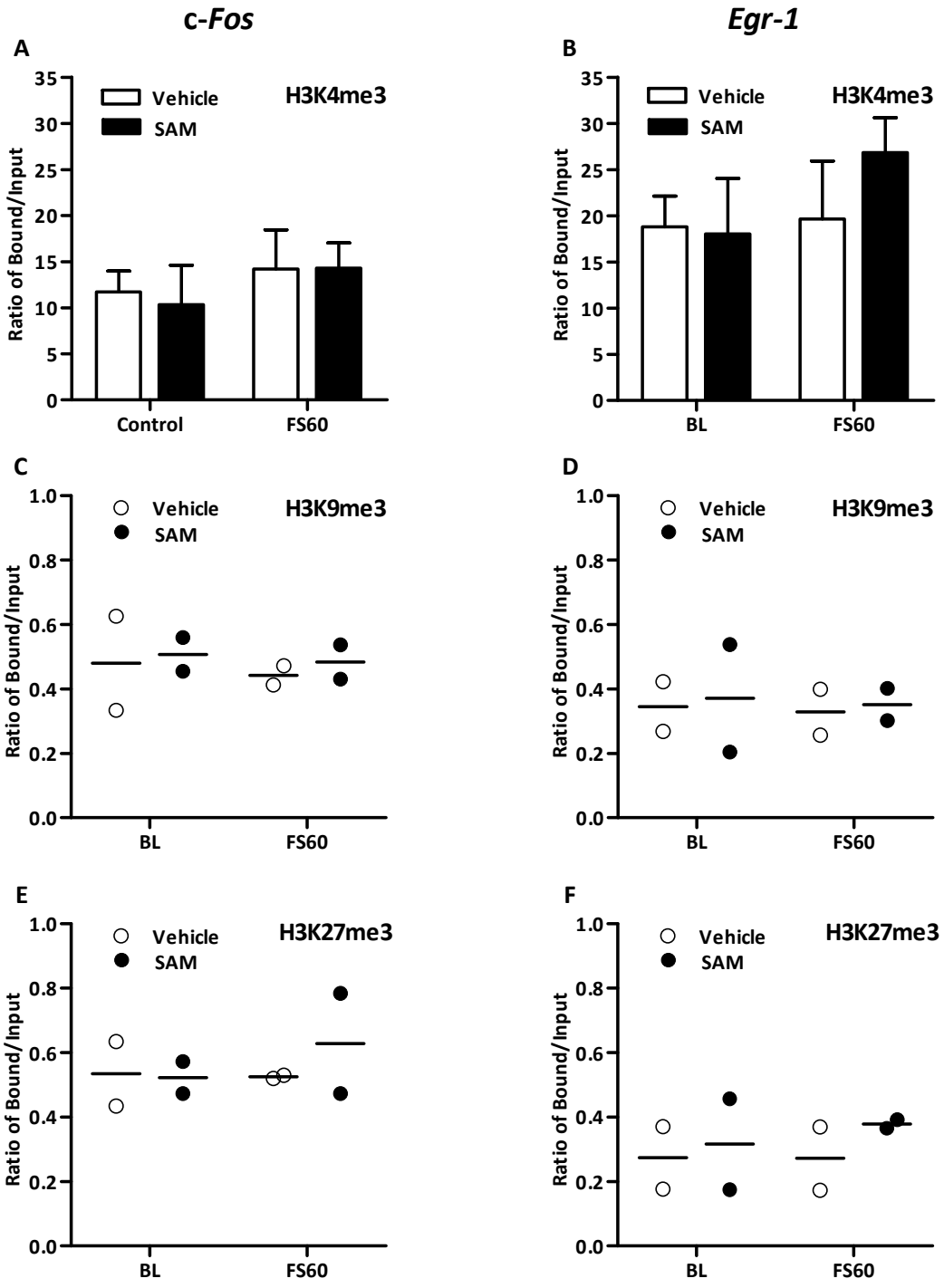
c-Fos
Egr-1
A
B
C
D
E
F
Vehicle
SAM
H3K4me3
H3K9me3
H3K27me3
Ratio of Bound/Input
Control
FS60
BL

Figure S9.

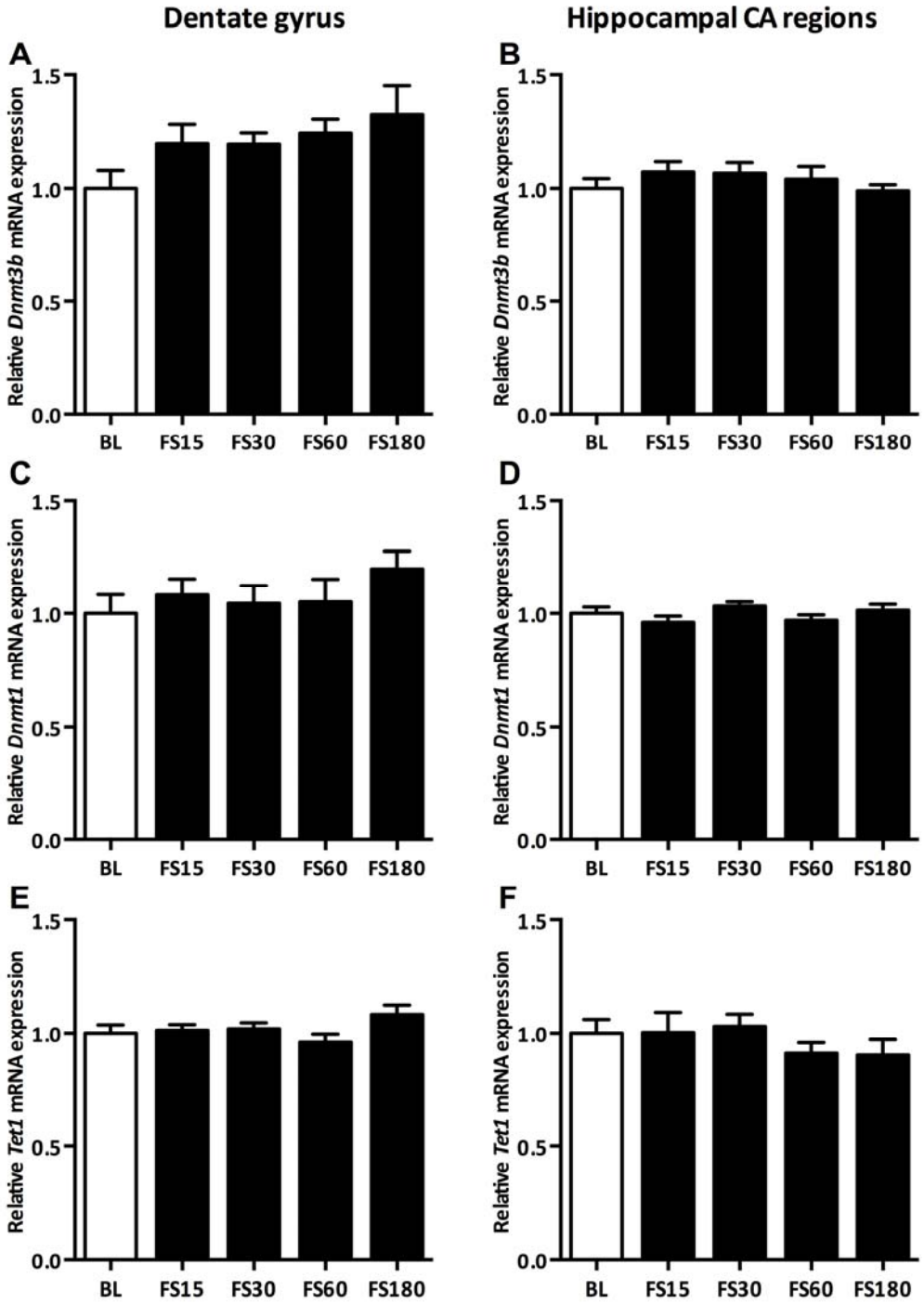
Dentate gyrus
Hippocampal CA regions
A
B
C
D
E
F
Relative Dnmt3b mRNA expression
Relative Dnmt1 mRNA expression
Relative Tet1 mRNA expression
1.5
1.0
0.5
0.0
BL
FS15
FS30
FS60
FS180